NORTHWESTERN UNIVERSITY

Downlink Packet Scheduling and Resource Allocation for Multiuser Video Transmission Over Wireless Networks

A DISSERTATION

SUBMITTED TO THE GRADUATE SCHOOL
IN PARTIAL FULFILLMENT OF THE REQUIREMENTS

for the degree

DOCTOR OF PHILOSOPHY

Field of Electrical Engineering and Computer Science

By

Peshala V. Pahalawatta

EVANSTON, ILLINOIS

December 2007

ABSTRACT

Downlink Packet Scheduling and Resource Allocation for Multiuser Video Transmission Over Wireless Networks

Peshala V. Pahalawatta

Video transmission over wireless networks to multiple mobile users has remained a challenging problem due to potential limitations on bandwidth and the time-varying nature of wireless channels. Recent advances in wireless access technologies, such as, HSDPA and IEEE 802.16, are targeted at achieving higher throughput over wireless networks. Meanwhile, advances in video compression, such as the recently developed H.264/AVC standard as well as scalable video coding schemes aim to provide more efficient video compression as well as increased adaptability to dynamic channel and network conditions.

This dissertation aims to benefit from the improving wireless access technologies and video compression standards by presenting cross-layer optimized packet scheduling schemes for the streaming of multiple pre-encoded video streams over wireless downlink packet access networks. A gradient based scheduling scheme is presented in which user data rates are dynamically adjusted based on channel quality as well as the gradients of a utility function. The user utilities are designed as a function of the distortion of the received video. This enables distortion-aware packet scheduling both within and across multiple users. In the

case of lossy channels with random packet losses, the utility functions are derived based on the expected distortion of the decoded video at the receiver. The utility takes into account decoder error concealment, an important component in deciding the received quality of the video. Both simple and complex decoder error concealment techniques are investigated.

Simulation results show that the gradient based scheduling framework combined with the content-aware utility functions provide a viable method for downlink packet scheduling as it can significantly outperform current content-independent techniques. Further tests determine the sensitivity of the system to the initial video encoding schemes, as well as to non-real-time packet ordering techniques. Comparisons are also made between scalable and conventional video coding techniques under the proposed schemes.

Acknowledgments

I would like to thank my father, Prof. P.D. Premasiri, and mother, Padma, for their support and wisdom without which I would never have reached this far. I would also like to thank my sisters, Vihanga and Sameerana, and of course, my entire extended family, including my late Seeya, Aachchi, and Kotte Aachchi, who have unconditionally supported me every step of the way. I would like to thank my wife, Kishwar Hossain, for her assistance in every aspect of my life, including some of the "artwork" for this dissertation.

I deeply appreciate the support given to me throughout my graduate career by my advisor, Prof. Aggelos Katsaggelos, as he patiently guided me towards this goal. I would also like to thank my co-advisors, Prof. Thrasyvoulos Pappas and Prof. Randall Berry, for their support and encouragement during this project. It has been a pleasure working with all my advisors at Northwestern, and their perspectives and insights are reflected in every aspect of this work. I would also like to thank Dr. Rajeev Agrawal and Hua Xu of the Network Advanced Technology group at Motorola for their valuable advice related to the applications of this work in industry.

I would like to thank my colleague Ehsan Maani whose collaboration resulted in the work related to packet lossy channels in this dissertation. I greatly value the insights and contributions resulting from the collaboration. I would like to thank my colleagues, Dr. Petar Aleksic and Dr. Sotirios Tsaftaris, for their advice, friendship, and support as I traveled back and forth from Champaign to complete my work. Many members, past and present, of the

Image and Video Processing Laboratory at Northwestern, have helped me in some manner along the way and I thank them all for their assistance and encouragement.

I also thank Prof. Allen Taflove and Dr. Nancy Anderson for the rewarding and fulfilling experience they provided me through the Residential College system at Northwestern University. Of course, I must also thank the many students of the Lindgren and Slivka residential colleges of science and engineering for always providing me with a fresh perspective that only an undergraduate can provide, even as I advanced deep into my graduate career.

Finally, I would like to thank the many benefactors who have helped me in the past, from my teachers at Trinity, to my "college guidance counselor", Mr. D.L.O. Mendis, to my teachers and advisors at Lafayette, especially, Prof. Ismail Jouny and Prof. David Hogenboom.

Table of Contents

List of Tables

List of Figures

CHAPTER 1

Introduction

1.1. Scope

The anticipated popularity of mobile multimedia devices drives wireless technology towards its third and fourth generation of development. Fourth generation (4G) networks are expected to provide higher data rates, and seamless connectivity, thus enabling users to access, store, and disseminate multimedia content without any restriction on mobility [**1**]. On-Demand video and video conferencing over mobile devices are among the many potential applications that stand to gain from the high data rates offered by such emerging wireless networks. The eventual success of such applications depends on the efficient management of system resources such as transmission power, bandwidth, and even time, in the case of scheduling of packets with attached delay constraints. To be efficient, the resource allocation schemes must also take into account the time-varying, and error-prone nature of wireless channels in a mobile environment, as well as the heterogeneous requirements of the transmitted multimedia content.

Any wireless video streaming system is composed of three high-level components. They are: 1) the server, which is either a media server that contains a collection of pre-encoded video sequences that can be requested by its clients, or a device that acquires video in real-time, compresses it, and then transmits the compressed video to its clients over the network; 2) the scheduler, which allocates the channel resources to be used for data transmission and

schedules the video packets; and 3) the clients that receive the data. It is becoming increasingly apparent that efficient video streaming schemes will require the consideration, and possibly the joint adaptation of source parameters, such as coding modes for macroblocks, at the encoder or server, and network and channel parameters, such as packet transmission schedules, and channel bandwidth allocations, at the scheduler, while also being aware of the video decoding and error resilience schemes employed at the receiving client [**2, 3, 4, 5**]. Jointly adapting such parameters, controls the allocation of the available resources across the multiple OSI network layers, from the application layer down to the physical layer. This dissertation introduces a cross layer resource allocation and packet scheduling scheme for multiuser video streaming over a downlink shared wireless channel. The work focuses on the real-time transmission of pre-encoded media where each user may be receiving a different video sequence with different characteristics from that of the other users. The resource allocation scheme takes into account the differences in video content, the concealability of errors in the video at the receiver, as well as the channel quality of each user. Furthermore, the video packets in the transmission buffer of each user are scheduled such that packets of greater importance will be given higher priority.

One of the key elements discussed in this work is that of error concealment at the decoder. Effective error concealment techniques have been developed in the video coding community to alleviate the ill-effects of losing individual slices of a video frame. They usually depend on utilizing the spatial and temporal correlations that exist between packets in compressed video [**6, 7**]. The exploitation of such correlations, however, introduces dependencies among otherwise independently decodable packets. Therefore, such dependencies must be taken into account in the packet scheduling scheme. The scheduling technique in this dissertation

assumes that the error concealment scheme used at the decoder is known and taken into account at the scheduler.

A major challenge in packet scheduling for real-time video transmission is the complexity involved in computing the packet priorities. The challenge is further magnified when error concealment is taken into account and the quality of service is measured in terms of the actual video quality rather than a content-independent metric such as packet loss rate. Schemes that compute video quality over multiple transmissions and packet loss realizations can be intractable due to the amount of computation required. Therefore the schemes discussed in this dissertation aim to limit computational complexity by reducing the required computation to only first order changes in video quality. In addition, techniques are shown that allow the first order changes to be calculated offline at the encoder, and signaled to the scheduler, thus significantly reducing the required computation at the scheduler.

This work also explores the use of scalable video coding techniques for application and channel dependent packet scheduling and resource allocation. Scalable video coding offers some natural advantages in terms of packet scheduling by limiting the dependencies between packets and thereby limiting the possibility of error propagation from dropped packets. This work explores some of the natural advantages to be had, and some pitfalls to be avoided, when using scalable coded video in conjunction with the proposed content-dependent scheduling and resource allocation. Also the performance of scalable coded video is compared to that of conventionally coded non-scalable video under varying channel conditions in order to determine the benefits of using the technique.

Whereas most of the proposed work is formulated under the assumption that perfect channel quality feedback is available at the scheduler, this dissertation also explores the challenges caused due to the availability of only delayed channel feedback. In that case,

since the exact channel conditions are not known, random packet losses can occur in the channel, and the exact quality of the reconstructed video at the decoder cannot be known at the scheduler. Work in this area has relied on calculating the expected distortion of the video at the decoder where the expectation is found with respect to the probability of loss of the transmitted packets [**8, 9, 5, 10**]. First order changes in the expected distortion are calculated in this work, to utilize a two-step strategy for scheduling and resource allocation in a wireless shared channel with random packet losses.

1.2. Background

1.2.1. Advancements in Wireless Access Technology

Since the inception of the digital cellular age with the introduction of the first GSM (Global System for Mobile communications) networks in Europe in 1991, there has been a rapid growth of interest in providing high speed data to mobile users over wireless networks. The main demand for high speed data comes from the need to supply multimedia content to mobile users. Multimedia content, and especially video, requires data rates in the order of a few hundred kilobits per second (kbps) in order to be of sufficient quality to be useful. In keeping with the rising demand for multimedia data transmission over wireless networks, the world's telecommunications bodies have also understood that the success of GSM lay at least partly in the effort to standardize the mobile communication platforms across regional and international boundaries. Thus, in 1996, the UMTS (Universal Mobile Telecommunications System) Forum was established in order to introduce a new generation of wireless digital communication standards that would lead to higher data rates, and ultimately, to multimedia communications. The HSDPA (High Speed Downlink Packet Access) standard, [**11**] is the latest standard to arise out of this effort.

The main features of HSDPA that differentiate it from its predecessors are the use of Wideband Code Division Multiple Access (WCDMA)[**12**] for channel sharing over multiple users combined with Time Division Multiplexing (TDM) with 2msec time slots, and packet-switched data transmission. These features along with the very high achievable throughput make HSDPA a very attractive standard for mobile multimedia communication and especially for video streaming applications.

One important characteristic that allows for greater efficiency in HSDPA is the ability to obtain channel quality feedback at 2msec intervals and to dynamically optimize the resource allocation decisions at a faster rate than previous standards. Faster adaptation to feedback is achieved by placing the MAC scheduler at the base station node and thereby reducing the feedback delay to the scheduler [**13**].

In addition to HSDPA, IEEE 802.16 (WiMAX) [**14, 15**] is another standard that promises to achieve significantly high data rates over wireless networks. IEEE 802.16 uses OFDMA (Orthogonal Frequency Division Multiple Access) instead of CDMA for bandwidth allocation. Some advantages of using OFDMA are that it allows for finer granularity in the bandwidth allocation, it offers the potential to tackle frequency selective channel fading, and it is easily scalable to the available bandwidth of the system [**16**]. In terms of allowing adaptive modulation and coding, and fast and frequent channel feedback, IEEE 802.16 is comparable to HSDPA, and therefore, the scheduling methods mentioned in this work can be adapted to both types of systems.

1.2.2. Scheduling and Resource Allocation in Wireless Networks

A number of cross-layer scheduling and resource allocation methods have been proposed that exploit the time-varying nature of the wireless channel to maximize the throughput of

the network. These methods rely on the multi-user diversity gain achieved by selectively allocating a majority of the available resources to users with good channel quality who can support higher data rates [**17, 18**]. While achieving high overall throughput, fairness across users must also be maintained in order to ensure that each user receives a reasonable quality of service. A number of schemes, which attempt to achieve such a balance can be found in [**19, 20, 21, 22, 23, 24**]. In [**19**], a fluid fair queueing model [**25**] is adapted to use with packet based data transmission and time varying wireless channels. The main purpose of the algorithm discussed in [**19**] is to readjust the service granted to each user at each transmission time window in order to ensure that users that were backlogged due to bad channel conditions will be given a greater share of the resources when their channel conditions improve. In [**20**], an *Exponential Rule*, is used where the priority of each user at each transmission time slot is determined as a function of the user's queue length and achievable data rate (which is a function of the channel state). A single user is allowed to transmit at each time slot. [**20**] analyzes the stability of such a rule in terms of maintaining quality of service and reducing delay. [**21**] discusses an algorithm that provides provable short-term fairness guarantees. Many of these opportunistic scheduling methods can be generalized as gradient-based scheduling policies [**26, 27**]. Gradient-based policies define a user utility as a function of some quality of service measure, such as throughput, and then maximize a weighted sum of the users' data rates where the weights are determined by the gradient of the utility function. For example, choosing the weights to be the reciprocals of the long term average throughput of each user, leads to a proportionally fair scheduling scheme [**23**]. Similarly, choosing the weights based on the delay of the head-of-line packet of each user's transmission queue leads to a delay-sensitive scheduling scheme [**24**]. A key characteristic of gradient based policies is that they rely on the instantaneous channel states

of each user in order to determine the resource allocations and do not assume any knowledge of the channel state distributions. In these policies, during each time-slot, the transmitter maximizes the weighted sum of each user's rate, where the (time-varying) weights are given by the gradient of a specified utility function. One attractive feature of such policies is that they require only myopic decisions, and hence, presume no knowledge of long-term channel or traffic distributions.

1.2.3. Video Compression Standards

While wireless data transmission standards have evolved towards providing greater throughput, the video coding community has also been in the process of evolving video coding standards in order to achieve higher compression rates while providing high quality video.

Almost all the widely accepted standards, including the successful MPEG 2 standard, use a block based hybrid motion compensated strategy for video encoding which allows spatial and temporal correlations in the video data to be exploited with limited computational complexity. This is done by temporally predicting image blocks from previously coded blocks in the video sequence, and transform coding the residual remaining after the prediction. Although the MPEG 2 standard [**28**], originally developed for digital television broadcasts, has remained a versatile standard due to its capacity to adapt to various applications and requirements, methods to improve compression efficiency and error resilience in video encoding have evolved significantly since its inception.

The latest standard to be specified through the effort to improve video encoding is that of H.264/AVC (Advanced Video Coding) [**29**]. The H.264/AVC standard, [**30**], first announced in 2002, is a collaborative effort of the International Telecommunication Union (ITU), the International Electrotechnical Commission (IEC) and the International Organization for

Standardization (ISO). This standard possesses multiple features that enable greater video compression rates while also introducing methods to improve the error resilience of transmitted data [**31**].

Some of the key features in H.264/AVC that lead towards greater compression efficiency and are also important to aspects of this work are briefly described below. More detailed explanations of each of these features can be found in [**29**].

- Variable Block Sizes for Motion Compensation: In H.264, inter (P) coded macroblocks (16x16 pel) can be partitioned into smaller blocks for the purposes of motion compensation. Then, each smaller block can be assigned a motion vector and reference picture. The smallest block size allowed is one containing 4x4 pixels, and therefore, each P coded macroblock can potentially contain up to 16 motion vectors. This feature enables more localized motion prediction and enables better exploitation of the temporal redundancies in the sequence during compression. This can also be an important feature when combined with temporal error concealment techniques that use the motion vectors of neighboring macroblocks to estimate motion vector of a lost macroblock. Since, each macroblock can contain up to 16 motion vectors, more flexibility is available in choosing a candidate concealment motion vector for a lost macroblock.
- Quarter Pixel Motion Estimation: The accuracy of motion estimation in H.264 is improved to quarter pixel resolution for the luminance component of the video signal. This is achieved by using a 6 tap FIR filter horizontally and vertically on the reference image prior to motion estimation in order to obtain the half pixel values, and then averaging the integer and half pixel values in order to estimate the pixel intensities at the quarter pixel locations. The chroma component is obtained using

bilinear interpolation. This allows for greater accuracy in motion compensation, and therefore, greater compression efficiency [**32**].

- In-Loop Deblocking Filter: Block based motion compensated video coding techniques suffer from visible compression artifacts at the block boundaries since the accuracy of reconstruction of pixels at the block boundaries is less than that of pixels towards the center of the block. In order to reduce such compression artifacts, H.264 uses an adaptive deblocking filter which is located within the hybrid motion compensation loop. In-loop refers to the fact that the deblocking filter is applied to each image prior to using the image as a reference for prediction of subsequent images in the sequence. The deblocking filter is adaptively applied in order to ensure that natural edges in the image will not be smoothed in the process. Overall, the deblocking filter also improves compression efficiency, since it generates a more accurate reference frame that can be used for motion compensation of subsequent frames [**33**].
- Intra Spatial Prediction: Another compression feature of H.264/AVC is that it uses spatial prediction from neighboring macroblocks for the encoding of intra (I) macroblocks. Pixel values from the macroblock directly to the left, and the one directly above the currently coded I macroblock are used to interpolate the predicted pixel values of the current I macroblock. Then, only the residual signal needs to be transform coded. While this form of prediction achieves greater compression efficiency, it can lead to error propagation if the spatially neighboring macroblocks are inter coded and use unreliable reference blocks for motion compensation. Therefore, in packet lossy channels, a constrained intra prediction mode, which stipulates that

only pixels from other intra coded macroblocks can be used for intra spatial prediction must be employed at the encoder [**31**].

- Prediction from B Frames: Unlike in previous video compression standards, H.264 allows for motion compensation of bi-predictive (B) frames from previously encoded B frames in the sequence. In addition to greater compression efficiency, this also enables temporal scalability through hierarchical bi-prediction, which is a useful feature for scalable video coding [**34**].

In addition to the improvements in compression noted above, H.264 also offers improvements in terms of robustness to error, which are important to consider in the context of wireless video streaming. Some of the more important error resilience features that are useful for this work are briefly described below.

- Parameter Set Structure: The parameter sets in H.264/AVC contain information that rarely needs refreshing during the decoding of the video sequence. A sequence parameter set contains information that applies to a sequence of coded pictures and a picture parameter set contains information that applies to one or more pictures within the sequence. The parameter sets are encapsulated in separate NAL (Network Abstraction Layer) units than the VCL (Video Coding Layer) data. Each VCL NAL unit can refer to a parameter set using the set's id, and therefore, multiple VCL NAL units can use the same parameter set.
- Flexible Slice Size: H.264 allows for flexible slice sizes, where the slices can contain any number of macroblocks in a picture. This is an important feature since some compression features such as predictive encoding of motion vectors and DCT coefficients cannot be used across slice boundaries. Therefore, larger slice sizes lead to

more efficient compression although smaller packet sizes allow greater flexibility in error concealment and loss protection.

- Arbitrary Slice Ordering: Each slice of a coded picture can be decoded independently of all other slices in the picture. Therefore, it should be possible for slices to be transmitted out of order, and yet be handled appropriately by an H.264 decoder. This is an important feature that is used extensively within this dissertation for prioritization of packets within the MAC layer transmission buffer.
- Data Partitioning: Some information such as macroblock types and motion vectors can be significantly more important for the purposes of generating a good quality decoded picture than others. Therefore, H.264 allows for data partitioning that will ensure that the more important data will be transmitted with higher priority. While this feature is not directly applied in this work, the prioritization methods discussed here can be easily generalized to the case of data partitioned sequences, as well.

Another important advancement in video compression standards has been that of improving the ability to develop scalable video bitstreams that offer progressive refinement of video quality by dynamically adapting the source rates to changing network and channel conditions. In the emerging scalable extension to the H.264 video coding standard, hierarchical bi-prediction (which is enabled by the ability in H.264 to predict from other B frames) or a wavelet based motion compensated temporal filtering method is used for progressive refinement of temporal resolution [**35, 36, 37**]. Quality (SNR) scalability of a given video frame can be obtained using a fine granularity scalability technique in which the transform coefficients of macroblocks are bit plane coded to obtain progressively finer resolution (smaller quantization step sizes) [**38, 39**]. Further details on the particular scalable video coding techniques investigated in this work are presented in Chapter 3.

1.2.4. Video Streaming Over Packet Access Networks

A wealth of work exists on video streaming in general, and on video streaming over wireless networks, in particular. One area, which has received significant attention has been that of optimal real-time video encoding, where the source content and channel model are jointly considered in determining the optimal source encoding modes [**40, 8, 41, 42, 43, 44**]. A thorough review of the existing approaches to joint source channel coding for video streaming can be found in [**5**]. The focus in this work, however, is on downlink video streaming where the media server is at a different location from the wireless base station, and the video encoding cannot be adapted to changes in the channel. Packet scheduling for the streaming of pre-encoded video is also a well-studied topic [**45, 46, 47**], where the focus has been on generating resource-distortion optimized strategies for transmission and retransmission of a pre-encoded sequence of video packets under lossy network conditions. The above methods, however, consider point-to-point streaming systems where a video sequence is streamed to a single client.

Packet scheduling for video streaming over wireless networks to multiple clients has conventionally focused on satisfying the delay constraint requirements inherent to the system. Examples of such work are [**48, 49**] and [**50**]. In these methods, the quality of service of the received video is measured only in terms of the packet delay, or packet loss rate.

Methods that do consider the media content can be found in [**51, 52, 53**]. In [**51**], a heuristic approach is used to determine the importance of frames across users based on the frame types (I, P, or B), or their positions in a group of pictures. In [**52**], a concept of incrementally additive distortion among video packets, introduced in [**45**], is used to determine the importance of video packets for each user. Scheduling across users, however,

is performed using conventional, content-independent techniques. In [**53**], the priority across users is determined as a combination of a content-aware importance measure similar to that in [**52**], and the delay of the *Head Of Line* (HOL) packet for each user. At each time slot, all the resources are dedicated to the user with the highest priority. It is important to note, however, that factors such as per user resource constraints or lack of available data, can make it advantageous to transmit to multiple users at the same time.

Multiuser streaming of scalable video has been considered in [**54**]. In [**54**], temporal scalability, in the form of hierarchical Bi-prediction [**55**], and SNR scalability, in the form of progressive refinement through fine granularity scalability (FGS) [**38**], is considered. A simple packet dropping strategy is used for buffer management and a maximum throughput scheduling strategy is used at the air interface.

1.3. Contributions

This work focuses on devising resource allocation strategies for the real-time transmission of pre-encoded video sequences to multiple users over TDM/CDMA, TDM/OFDMA type wireless networks in which the resources allocated to each user can be adapted at each transmission opportunity. The work utilizes some of the new features of emerging wireless standards as well as improvements in video compression standards in order to devise content-dependent video packet scheduling and resource allocation strategies for multiuser video communication. The ability to transmit streaming video content to multiple users could potentially enable users to view news telecasts, streamed sports telecasts, etc, at high quality on demand, from media content servers, through their mobile devices. Another motivation for considering video streaming systems is that the drive by consumers to demand smaller mobile phones essentially limits the capacity of phones to buffer large amounts of data. Other

considerations such as copyrights on the content may also prompt media content servers to require video streaming systems.

The main contributions of this work lie in the video packet prioritization strategies and distortion based resource allocation strategies that will enable the transmission of video packets over wireless networks to multiple mobile users where the achievable data rates may not be sufficient for the transmission of the complete coded bitstreams. The resource allocation scheme departs from the schemes discussed in Sec. 1.2.4 in that it is performed at each transmission time slot based only on the instantaneous channel fading states of each user. A content-based utility function is proposed in which the gradients of the utility function can be used in conjunction with the gradient-based scheduling schemes proposed in [**26**]. The method orders the encoded video packets by their relative contribution to the final quality of the video, and assigns a utility for each packet, which can then be used by the gradient-based scheduling scheme to allocate resources across users.

Decoder error concealment, which can significantly affect the importance of video packets, is explicitly taken into account in the formulation, and the effect of dependencies introduced between video packets as a result of decoder error concealment is also considered.

Packet prioritization schemes for scalable coded video are also considered and methods are proposed that determine the packet prioritization strategy such that the distortion based utility functions obtained after prioritization are amenable to the gradient-based resource allocation strategies proposed in this work.

In the case when packet losses in the channel are random due to channel fading, the proposed scheme is generalized to use the expected distortions calculated at the transmitter where the expectation is calculated with regard to the packet loss probabilities in the channel.

1.4. Organization

The next chapter provides the general formulation for gradient based scheduling and resource allocation using a content-dependent utility function. The scheme is compared to a conventional content-independent technique, and also the performance of the scheme is demonstrated for the case when simple and complex error concealment techniques are used at the decoder. Other important aspects of the problem such as error resilient encoding methods and real time versus offline packet scheduling schemes are also discussed in the chapter.

Chapter 3 extends the algorithms presented in Chapter 2 to scalable video encoding schemes. Packet prioritization schemes that perform well in conjunction with the gradient based resource allocation framework are presented, and again, comparisons are made between content dependent and content-independent scheduling. The scalable schemes are also compared against the less flexible conventional video coding schemes.

In Chapter 4, the problem is extended to the case when perfect channel state information is not available to the scheduler. In that case, random packet losses can occur in the channel, and an expected distortion based utility needs to be calculated at the transmitter. A two step solution is presented that jointly optimizes the resource allocation parameters in the channel as well as the transmission rate in order to minimize the overall expected distortion at the multiple receivers.

Chapter 5 presents a summary and the main conclusions of this work. Some avenues for future work are also discussed.

CHAPTER 2

Packet Scheduling and Resource Allocation for Video Transmission

This section describes the general system under consideration and formulates the problem in terms of the resources and constraints pertaining to the system. The section ends with a simulation study detailing the performance of the resource allocation scheme under various conditions such as decoder error concealment techniques, error resilient encoding, and offline packet ordering.

2.1. System Overview

Figure 2.1 provides a high-level overview of the multiuser wireless video streaming system. The system begins at a media server containing multiple video sequences. The server consists of a media encoder, which, along with data compression, also packets each video sequence into multiple *data units*. Each data unit/packet is independently decodable and represents a *slice* of the video. In recent video coding standards, such as H.264, a slice can either be as small as a group of a few macroblocks (MBs), or as large as an entire video frame. Each slice header acts as a resynchronization marker, which enables the decoder to independently decode each slice. In H.264, the encoder can also transport the slices out of order (Arbitrary Slice Ordering) without affecting the decoder's ability to decode each slice [**30**]. Note that, although in terms of decoder operation, each slice is independently decodable, in reality, most frames of a compressed sequence are inter frames, in which MBs can be predictively

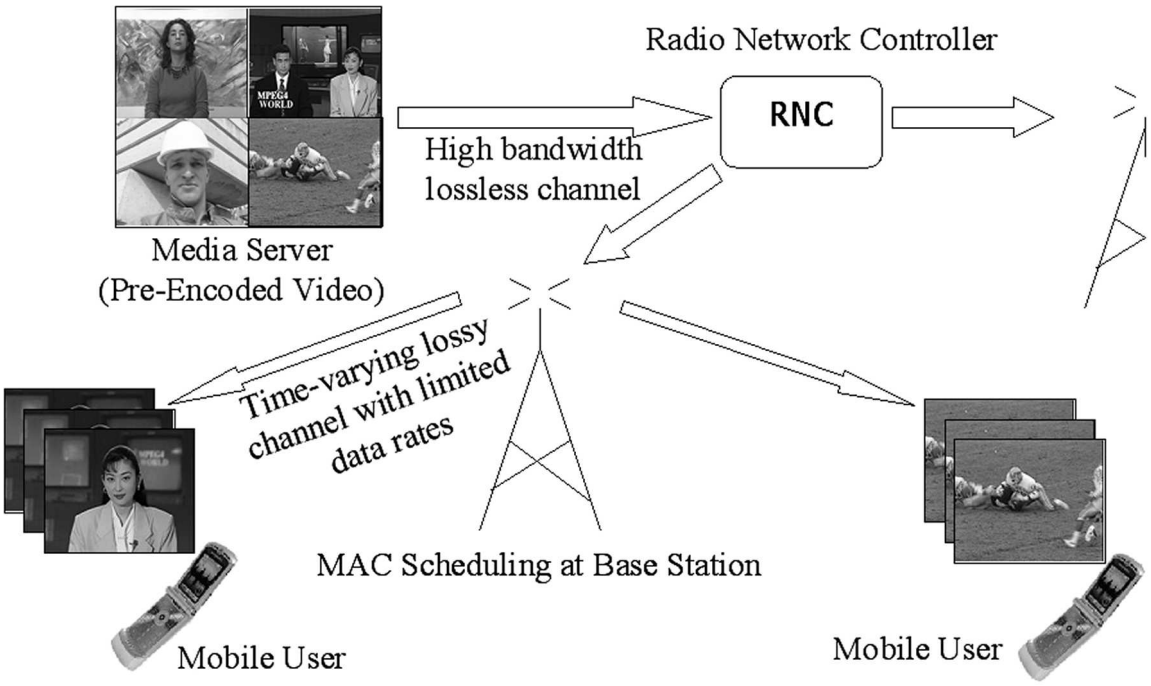

Figure 2.1. Overview of multiuser downlink video streaming system

dependent on macroblocks of previous frames through motion estimation. Therefore, when the transmitter drops packets due to congestion, or when packets are lost in the channel, the errors at the decoder can propagate to other received packets in the sequence.

Once a client requests a video stream, the media server transmits the video packets over a backbone network to the scheduler at a base station servicing multiple clients. This work assumes that the backbone network is lossless and of high bandwidth. For clarity, this work assumes that the base station serves only video users. The scheduling rule, however, can easily accommodate other, non-video, users by assigning them different utility functions. The scheduler uses three features of each packet, in addition to *Channel State Information* (CSI) available through channel feedback, to allocate resources across users. They are, for each packet m of each client i, the utility gained due to transmitting the packet (described in Sec. 2.2), the size of the packet in bits, $b_{i,m}$, and the decoding deadline for the packet,

$\tau_{i,m}$. The decoding deadline, $\tau_{i,m}$, stems from the video streaming requirement that all the packets needed to decode a frame of the video sequence must be received at the decoder buffer prior to the playback time of that frame. Multiple packets (e.g., all the packets in one frame) can have the same decoding deadline.

The transmitter must drop any packet left in the transmission queue after the expiration of the packet's decoding deadline. Assuming real-time transmission, the number of transmission time slots available per each video frame can be calculated from the playback time for a frame (approximately 33msec for 30fps video), and the length of each time-slot (e.g., 2msec for HSDPA). Note that, unlike video conferencing systems, video streaming applications can afford some buffer time at the decoder before starting to play back the video sequence. This is important because, in a compressed sequence, the quality of the first frame, which is intra coded, can have a significant impact on the quality of the following inter coded frames of the same sequence.

The next step in Fig. 2.1 is that of receiving and decoding the video. At this point, the decoded picture can contain numerous errors due to the loss of packets in the wireless channel, or due to the dropping of packets from the transmission queue. Typically, the decoder attempts to conceal these errors using an appropriate error concealment technique. In general, error concealment techniques use spatial and temporal correlations in the video data. The decoder estimates the pixel values of macroblocks represented by lost slices using data from the received slices of the current and/or reference frame. Therefore, error concealment introduces an additional dependency between the slices of the sequence [**6, 7**].

2.2. A Content Aware Utility Function and Its Gradient

The main contribution of this work is to propose a utility function for video streaming that accounts for both the dependencies between individual video packets, and the effect that each video packet has on the final quality of the received video. The proposed utility function is especially relevant since it can be used in conjunction with the gradient-based scheduling scheme of [**26**] to enable content-aware resource allocation across multiple users. In gradient-based scheduling algorithms, the scheduler assigns greater priority to packets with a larger first-order change in utility. The key idea in the proposed method is to sort the packets in the transmission buffer for each user based on the contribution of each packet to the overall video quality, and then, to construct a utility function such that its gradient reflects the contribution of each packet. A description of the process used to generate packet utilities is given below.

At a given transmission time slot, t, for each user, i, pick a group of M_i available packets such that each packet m in M_i has a decoding deadline, $\tau_{i,m}$, greater than t. An obvious approach would be to pick the group of packets with the same decoding deadline that compose the current frame, or group of frames, to be transmitted. Each packet m consists of $b_{i,m}$ bits. Note that, since the optimization is performed on a per time-slot basis, the time index, t, remains the same throughout one optimization period, and therefore, is omitted for the purposes of this discussion. Now, let $\Pi_i = \{\pi_{i,1}, \pi_{i,2}, ..., \pi_{i,M_i}\}$ be the re-ordered set of packets in the transmission queue of user i such that the transmitter will send packet $\pi_{i,1}$ first, packet $\pi_{i,2}$ second, and so on. Let $D_i[\{\pi_{i,1}, \pi_{i,2}, ..., \pi_{i,k_i}\}]$ denote the distortion given that the transmitter sends the first k_i packets in the queue to user i and drops the remaining $(M_i - k_i)$ packets prior to transmission. Then, define the user utility for user i after k_i packet

transmissions as,

$$U_i[k_i] = (D_i[\Pi_i] - D_i[\{\pi_{i,1}, \pi_{i,2}, ..., \pi_{i,k_i}\}]), \tag{2.1}$$

where $D_i[\Pi_i]$ is the minimum distortion for the frame, which occurs if the decoder receives all of the packets in the group. Note that the scheduler will need to calculate a new utility function only after it sends all M_i packets in the queue, or after it determines that the decoding deadlines of all M_i packets have expired. The proposed scheme does not depend on the metric used to calculate the distortion. For numerical simplicity, this work defines the distortion as either the sum absolute pixel difference (SAD) or mean-squared error (MSE) between the decoded and error-free frames. For ease of notation, let $\Pi_i(k_i) = \{\pi_{i,1}, ..., \pi_{i,k_i}\}$. Then, assuming a simple error concealment scheme (as described in Sec. 2.5.1), the scheduler can guarantee that the user utility function is concave and increasing by iteratively choosing each additional packet π_{i,k_i+1} in a manner that maximizes the utility gradient; i.e.,

$$\pi_{i,k_i+1} = \arg \max_{m \notin \Pi_i(k_i)} u_{i,m}[k_i], \tag{2.2}$$

where,

$$u_{i,m}[k_i] = \frac{D_i[\Pi_i(k_i)] - D_i[\{\Pi_i(k_i), m\} \,|\Pi_i(k_i)]}{b_{i,m}}. \tag{2.3}$$

In (2.3), $D_i[\{\Pi_i(k_i), m\} \,|\Pi_i(k_i)]$ indicates that the distortion after adding packet m may be dependent on the currently ordered set of packets $\Pi_i(k_i)$ from the same group. This will be true if the decoder uses a complex error concealment technique to recover from packet losses (See Sec. 2.5.2).

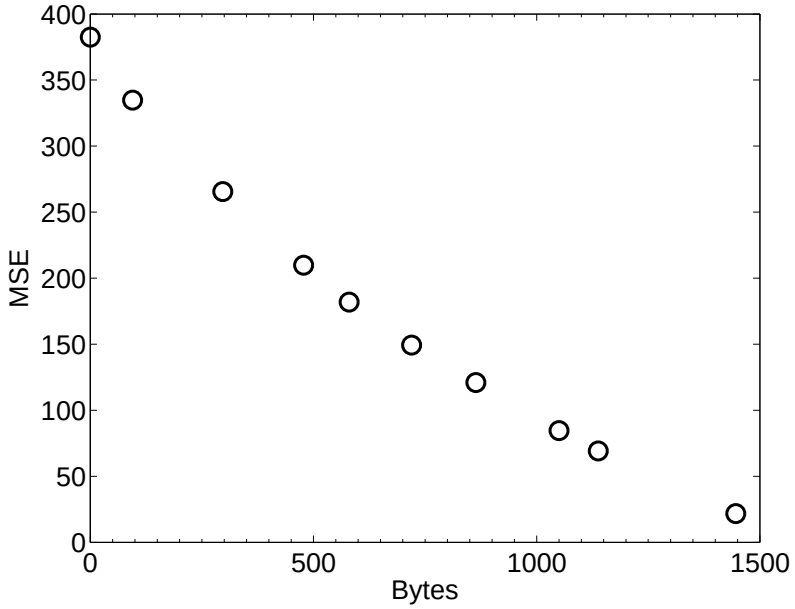

Figure 2.2. Distortion as a function of transmitted packets for a frame from the foreman sequence with simple error concealment. The markers indicate packet boundaries.

Figures 2.2 and 2.3 illustrate the generation of the utility function. Figure 2.2 shows the distortion of a frame in the foreman sequence as a function of the number of received packets from the frame, where the packets have already been ordered by their utility gradients. Since each packet can be of a different length in bytes, the x-axis depicts the number of bytes transmitted. Then, the utility function in Fig. 2.3 can be easily generated from Fig. 2.2. The utility gradients, of each user correspond to the slope of the utility function, which is equal to the reduction in distortion per bit due to transmitting the next packet in the ordered set.

The proposed technique uses the utility gradients, $u_{i,\pi_{i,k_i+1}}[k_i]$, with the gradient-based scheduling framework in Sec. 2.3.3 to ensure that the resource allocation will explicitly consider the improvements in video quality for each user.

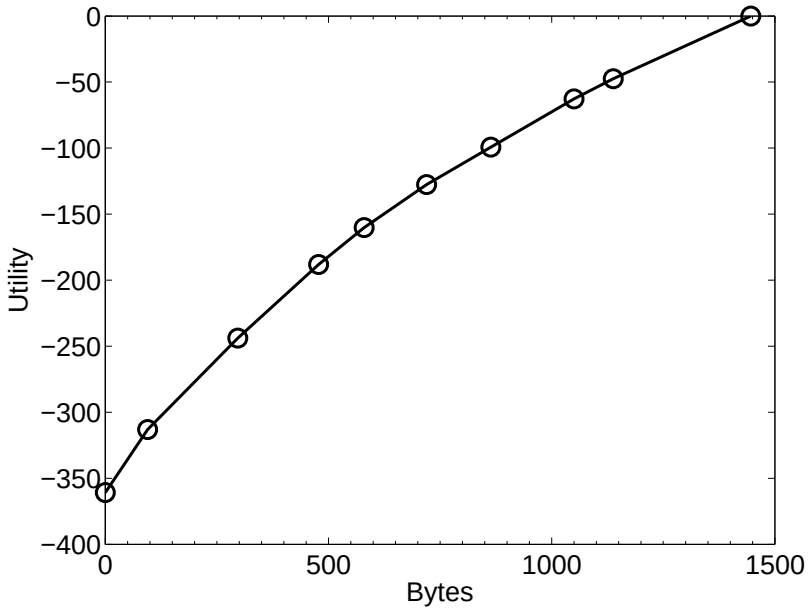

Figure 2.3. Utility function for the frame.

2.3. Problem Formulation

2.3.1. Channel Resources and Constraints

For numerical purposes, this work considers a scheme where a combination of TDM and CDMA is used, in which at a given transmission opportunity, t, the scheduler can decide on the number of spreading codes, n_i, (assumed to be orthogonal) that can be used to transmit to a given user, i. Note that $n_i = 0$ implies that user i is not scheduled for transmission at that time slot (as in the previous section, the time-slot index remains the same throughout this section and is omitted for simplicity). The maximum number of spreading codes that can be handled by each user is determined by the user's mobile device. However, the total number of spreading codes, N, that can be allocated to all users, is limited by the specific standard ($N = 15$ for HSDPA). In addition to the number of spreading codes, the scheduler can also decide on the power level, p_i, used to transmit to a given user. The total power,

P, that can be used by the base station is also limited in order to restrict the possibility of interference across neighboring cells. Assuming K total users, these constraints can be written as:

$$\sum_{i=1}^{K} n_i \leq N, \quad \sum_{i=1}^{K} p_i \leq P, \quad \text{and, } n_i \leq N_i, \tag{2.4}$$

where N_i is the maximum number of spreading codes for user i.

The basic assumption in this work is that the constraints of the system will be such that the transmitter may not be able to transmit all the available video packets in the transmission queue of each user in time to meet their decoding deadlines.

2.3.2. General Problem Definition

Assume that the channel state for user i, denoted by e_i, at a given time slot is known based on channel quality feedback available in the system. The case when only imperfect channel state information is known at the scheduler will be discussed in Chapter 4. The value of e_i represents the normalized *Signal to Interference Plus Noise Ratio* (SINR) per unit power and can vary quite rapidly, and in a large dynamic range, over time. Therefore, it is reasonable to assume that e_i will be a different value at each time slot. Defining $SINR_i = \frac{p_i}{n_i} e_i$ to be the SINR per code for user i at a given time, the achievable rate for user i, r_i, satisfies:

$$\frac{r_i}{n_i} = \Gamma(\zeta_i SINR_i). \tag{2.5}$$

In (2.5), $\Gamma(x) = B\log(1+x)$ represents the Shannon capacity for an AWGN channel, where B is the symbol rate per code. Also, $\zeta_i \in (0, 1]$ represents a scaling factor that determines the *gap from capacity* for a realistic system. This is a reasonable model for systems that use

coding techniques, such as turbo codes, that approach Shannon capacity. Setting $\breve{e}_i = e_i\zeta_i$, the achievable rates for each user as a function of the control parameters n_i and p_i can be specified as follows:

$$r_i = n_i B \log\left(1 + \frac{p_i \breve{e}_i}{n_i}\right) \tag{2.6}$$

Now, the resource allocation problem becomes one of specifying the n_i and p_i allocated to each user such that a target rate, r_i, can be achieved.

2.3.3. Gradient-Based Scheduling Framework

The key idea in the gradient-based scheduling technique is to maximize the projection of the achievable rate vector, $\mathbf{r} = (r_1, r_2, ..., r_K)$ on to the gradient of a system utility function [**26**]. The system utility function is defined as:

$$\mathbf{U}_i = \sum_{i=1}^{K} U_i, \tag{2.7}$$

where U_i is a concave utility function. In a content-independent scheme, U_i can be a function of the average throughput for user i, or the delay of the head-of-line packet. The proposed content-aware scheme, however, defines U_i to be a function of the decoded video quality as in (2.1). Now, the gradient based resource allocation problem can be written as:

$$\max_{\mathbf{r}\in\mathcal{C}(\breve{\mathbf{e}},\chi)} \sum_{i=1}^{K} w_i u_{i,\pi_{i,k_i+1}}[k_i] r_i \tag{2.8}$$

where, as in (2.3), k_i denotes the number of packets already transmitted to user i, and π_{i,k_i+1} denotes the next packet in the ordered transmission queue. The constraint set, $\mathcal{C}(\breve{\mathbf{e}}, \chi)$, denotes all the achievable rates given $\breve{\mathbf{e}}$, the vector containing the instantaneous channel

states of each user, and χ the set of allowable $\mathbf{n} = (n_1, n_2, ..., n_K)$ and $\mathbf{p} = (p_1, p_2, ..., p_K)$, the vectors containing the assigned number of spreading codes, and assigned power levels, of each user, respectively. Here, w_i indicates an additional weighting used to attain fairness across users over time. This work considers a content-based technique for determining w_i based on the distortion in user i's decoded video given the previously transmitted set of packets (i.e., user's with poor decoded quality based on the previous transmissions will be assigned larger weights in order to ensure fairness over time). In that case, w_i will also be a function of k_i.

The formulation in (2.8) maximizes a weighted sum of the rates assigned to each user where the weights are proportional to the gradients of the system utility function. After each time-slot, k_i will be updated, and the weights will be re-adjusted based on the packets scheduled in the previous slot. The constraint set will also change at each time-slot due to changes in the channel states.

Now, taking into account the system constraints specified in (2.4), as well as the formula for calculating each user's achievable rate specified in (2.6), the optimization problem formulation becomes:

$$V^* := \max_{(\mathbf{n},\mathbf{p})\in\chi} V(\mathbf{n},\mathbf{p}), \tag{2.9}$$

subject to:

$$\sum_{i=1}^{K} n_i \leq N, \qquad \sum_{i=1}^{K} p_i \leq P,$$

where:

$$V(\mathbf{n},\mathbf{p}) := \sum_{i=1}^{K} w_i u_{i,\pi_{i,k_i+1}}[k_i] n_i \log\left(1 + \frac{p_i \breve{e}_i}{n_i}\right), \tag{2.10}$$

and,

$$\chi \;:=\; \{(\mathbf{n},\mathbf{p}) \geq 0 : n_i \leq N_i \;\forall i\}. \tag{2.11}$$

2.3.4. Additional Constraints

In addition to the main constraints specified above, a practical system is also limited by some "per-user" constraints. Among them are, a peak power constraint per user, a maximum SINR per code constraint for each user, and a maximum and minimum rate constraint determined by the maximum and minimum coding rates allowed by the coding scheme.

All of the above constraints can be grouped into a *per user power constraint* based on the SINR per code for each user [**26**]. This constraint can be viewed as:

$$SINR_i = \frac{p_i \breve{e}_i}{n_i} \in [\breve{s}_i(n_i), s_i(n_i)]\,,\ \forall i, \tag{2.12}$$

where $\breve{s}_i(n_i) \geq 0$. For the purposes of this work, only cases where the maximum and minimum SINR constraints are not functions of n_i, i.e, $SINR_i \in [\breve{s}_i, s_i]$, as with a maximum SINR per code constraint, are considered. In this case, the constraint set in (2.11) becomes,

$$\chi := \{(\mathbf{n},\mathbf{p}) \geq 0 : n_i \leq N_i,\ \breve{s}_i \leq \frac{p_i \breve{e}_i}{n_i} \leq s_i \;\forall i\}. \tag{2.13}$$

2.3.5. Extension to OFDMA

Although the above formulation is primarily designed for CDMA systems, it can also be adapted for use in OFDMA systems under suitable conditions. For example, a common approach followed in OFDMA systems, is to form multiple *subchannels* consisting of sets of OFDM tones. In the case that the OFDM tones are interleaved to form the subchannels (i.e.,

interleaved channelization is used), which is the default case, referred to as PUSC (Partially Used SubCarrier), in IEEE 802.16d/e [**14**], the SINR is essentially uniform across all the subchannels for each user. Then, the number of subchannels plays an equivalent role to the number of codes (N) in the CDMA based formulation above. Further details on gradient based scheduling approaches with OFDMA can be found in [**56**].

2.4. Solution

A solution to the convex optimization problem of the type given in (2.9) for the case when the maximum and minimum SINR constraints are not functions of n_i is derived in detail in [**26**]. This section simply summarizes the basic form of the solution.

The Lagrangian for the primal problem in (2.9) can be defined as:

$$\begin{aligned} L(\mathbf{p},\mathbf{n},\lambda,\mu) = & \\ & \sum_i w_i u_i n_i \log\left(1+\frac{p_i \breve{e}_i}{n_i}\right) + \\ & \lambda\left(P-\sum_i p_i\right)+\mu\left(N-\sum_i n_i\right). \end{aligned} \tag{2.14}$$

Based on this, the dual function can defined as,

$$L(\lambda,\mu) = \max_{(\mathbf{n},\mathbf{p})\in\chi} L(\mathbf{p},\mathbf{n},\lambda,\mu), \tag{2.15}$$

which can be analytically computed by first keeping $\mathbf{n},\lambda,\mu$ fixed and optimizing (2.14) over $\mathbf{p}$, and then optimizing over $\mathbf{n}$.

The corresponding dual problem is given by,

$$L^* = \min_{(\lambda,\mu)\geq 0} L(\lambda,\mu). \tag{2.16}$$

Based on the concavity of V in (2.9), and the convexity of the domain of optimization, it can be shown that a solution to the dual problem exists, and that there is no duality gap, i.e., $V^* = L^*$.

In [**26**], an algorithm is given for solving the dual problem based on first optimizing over μ for a fixed λ to find,

$$L(\lambda) = \max_{\mu \geq 0} L(\lambda, \mu), \tag{2.17}$$

and then minimizing $L(\lambda)$ over $\lambda \geq 0$. For the first step, $L(\lambda)$ can be analytically computed. The function $L(\lambda)$ can be shown to be a convex function of λ, which can then be minimized via a one-dimensional search with geometric convergence.

2.5. Simulation Study

This section will detail some of the characteristics of the proposed technique based on simulations performed using an experimental multiuser wireless video streaming setup. Minor modifications are also proposed in order to adapt the scheme to realistic conditions such as complex error concealment techniques, fragmentation at the MAC layer, and offline packet ordering.

Six video sequences with varied content: "foreman", "carphone", "mother and daughter", "news", "hall monitor", and "silent", in QCIF (176x144) format were used for the simulations. The sequences were encoded in H.264 (JVT reference software, JM 9.3 [**57**]) at variable bit rates to obtain a specified average PSNR of 35dB for each frame. All frames except the first were encoded as P frames. To reduce error propagation due to packet losses, random I MBs were inserted into each frame during the encoding process. The frames were

Table 2.1. System Parameters Used in Simulations

N	N_i	P	$\breve{s}_i$	s_i
15	5	10W	0	1.76dB

packeted such that each packet/slice contained one row of MBs, which enabled a good balance between error robustness and compression efficiency. Constrained intra prediction was used at the encoder for further error robustness. Although the sequences begin transmitting simultaneously, a buffer of 10 frame times was provided in order for the first frame (Intra coded) to be received by each user. Therefore, the start times of the subsequent frames could vary for each user. If a video packet could not be completely transmitted within a given transmission opportunity, it was assumed to be fragmented at the MAC layer, and the utility gradient of the fragmented packet was calculated using the number of remaining bits to be transmitted for that packet.

The wireless network was modeled as an HSDPA system. The system parameters used in the simulations are shown in Table 2.1. HSDPA provides 2 msec transmission time slots. Realistic channel traces for an HSDPA system were obtained using a proprietary channel simulator developed at Motorola Inc. The simulator accounts for correlated shadowing and multipath fading effects with 6 multipath components. For the channel traces, users were located within a 0.8km radius from the base station and user speeds were set at 30km/h.

2.5.1. Simple Error Concealment

The error concealment technique used at the decoder significantly impacts the reconstructed state of a decoded video frame after packet losses. The decoder has access to only its own, possibly distorted, reconstructed frames for motion compensation of subsequent received predictive frames. Any errors in the reconstruction of a frame at the decoder can propagate

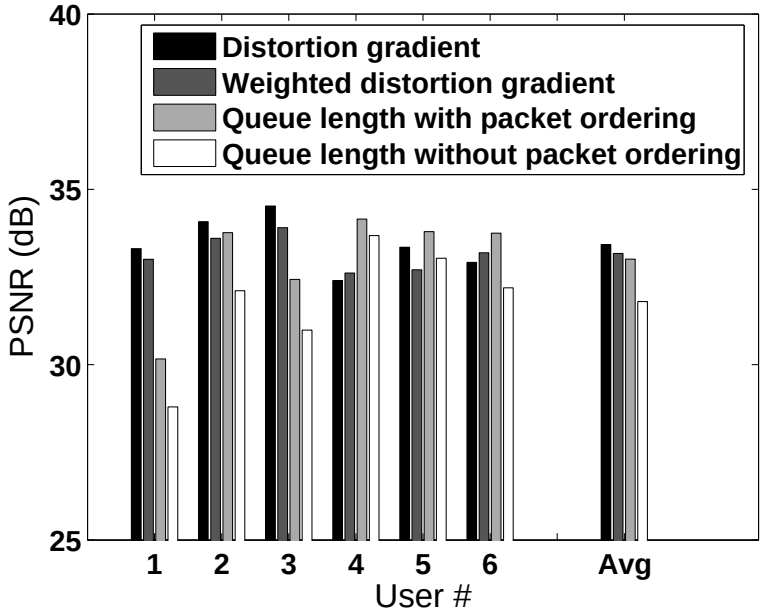

Figure 2.4. Comparison of average PSNR with resource allocation schemes using simple error concealment. User numbers represent 1: Foreman, 2: Mother and Daughter, 3: Carphone, 4: News, 5: Silent, 6: Hall Monitor.

to future frames, as well, due to the predictive dependencies among frames. Therefore, the error concealment at the decoder, and thereby, the reconstructed states of frames at the decoder must be taken into account when determining the importance of video packets. A number of error concealment techniques for packet based video have been proposed in the literature. For the purposes of this work, they can be categorized as "simple" and "complex" concealment techniques.

A *simple* concealment scheme can be categorized as any error concealment technique, in which data from packets within the same group, Π_i, are not used for concealment of other lost packets within that group. For example, if each group consists of packets from one video frame, then replacing the pixel values of MBs contained on a lost packet with pixel values from the same location in the previous frame is a commonly used simple error concealment

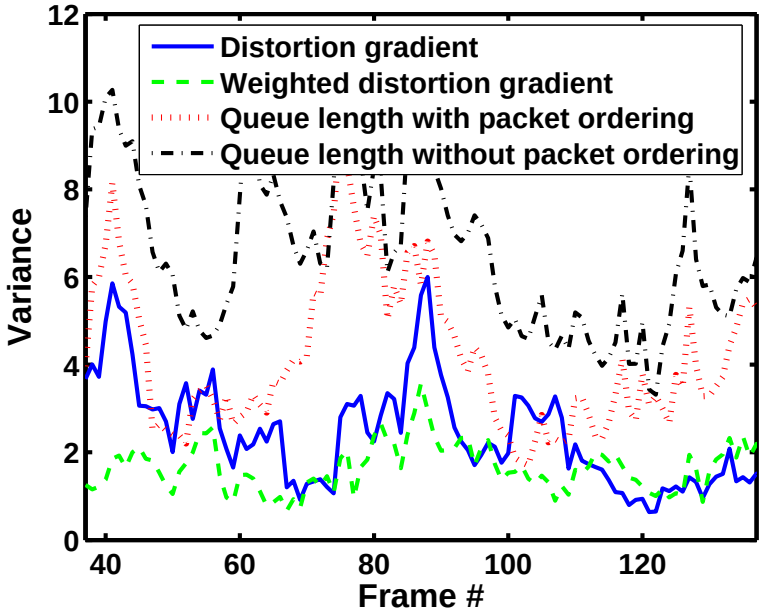

Figure 2.5. Comparison of variance of PSNR with resource allocation schemes using simple error concealment.

technique. With such techniques, it can be seen that the packet ordering scheme proposed in Sec. 2.2 will always provide the best possible ordering of packets within a packet group, such that given only k_i out of the total M_i packets are actually transmitted, $\Pi_i(k_i)$ would be the set of packets that would lead to the highest decoded video quality. In concise terms, with simple concealment, the packet ordering within a given packet group does not depend on the channel realizations during the transmission of that packet group. Also, it can be guaranteed that the contribution per bit of each newly transmitted packet from the group will be lower than that of the previously transmitted packet, and that therefore, the utility function will be concave.

Simulations were performed, using the simple error concealment technique described above, to determine the performance gain that can be expected by using the content-dependent packet ordering and resource allocation scheme. Figures 2.4 and 2.5 compare

the quality of the received video, using 4 different methods for calculating the utilities in (2.8). They are:

(1) Distortion Gradient - This method uses the packet ordering and utility functions described in Sec. 2.2 but sets $w_i = 1$ for all i in (2.10). Essentially this method attempts to minimize the total distortion over all users without regard to fairness for individual users.

(2) Weighted Distortion Gradient - This method is similar to the first but it sets w_i to be the distortion in user i's decoded video frame given the packets transmitted up to that point. This ensures that users that are suffering from degraded performance due to effects of channel fading in previous time slots will be given a higher priority in the current time slot.

(3) Ordered Queue Length - This method is only partially content-aware in that it orders the video packets of each user according to their importance. The resource allocation across users, however, is performed assuming that the utility gradients in (2.8) are proportional to the current queue length in bits of each user's transmission queue. The resource allocation is similar to the M-LWDF scheme in [**24**].

(4) Queue Length - The final method is a direct application of the conventional content-independent scheduling technique, again essentially the M-LWDF scheme, without performing any packet ordering at the scheduler.

The computational complexity of the first three methods is very similar as they all use the proposed packet ordering scheme. Assuming simple error concealment, and that the packet group consists of the packets of one frame, the packet ordering requires one decoding of the entire video frame, a calculation of the distortion gradients of each packet, and a sort over

the number of packets. Due to concealment from the previous frame, the calculation of the distortion gradients requires that the previous decoded frame, i.e., the reconstructed frame based on the number of packets transmitted from the previous frame, be kept in memory. The fourth method is less computationally complex as it does not require packet ordering.

Figure 2.4 shows the average quality across 100 frames over 5 channel realizations for each sequence. This shows that the content-aware schemes significantly out-perform the conventional queue length based scheduling scheme. The gain in performance is mainly seen in the sequences with more complex video content across the entire frame such as foreman, mother and daughter, and carphone. The content aware schemes recognize the importance of error concealment in enabling packets in more easily concealable sequences such as news and hall monitor to be dropped, while the content-independent schemes do not. Figure 2.5 shows the variance in PSNR per frame across all users and the 5 channel realizations. This shows that the two schemes with content-aware gradient metrics tend to provide similar quality across all the users (lower variance), while the queue-dependent schemes tend to favor some users, again those whose dropped packets would have been easily concealable, over others. Between the two schemes with content-aware metrics, a small sacrifice in average PSNR incurred by the weighted distortion gradient metric yields significant improvement in terms of the variance across users.

2.5.2. Complex Error Concealment

A broad review of error concealment techniques can be found in [**58, 7**]. Error concealment exploits spatial and temporal redundancies in the video data. In complex temporal concealment techniques, the motion vectors (MV's) of neighboring decoded MB's in the same frame are used to estimate the motion vector of a lost MB. For example, one possibility is

to use the median MV of all the available neighboring MV's. Another is to use a boundary matching technique to determine the best candidate MV [**59**]. Errors in intra frames are concealed using spatial concealment techniques that rely on weighted pixel averaging schemes where the weight depends on the distance from the concealed pixels. More complex hybrid spatio-temporal error concealment techniques also exist[**60**].

When complex concealment is used, the packet ordering scheme proposed in Sec. 2.2 changes, and the incremental gain in quality due to adding each packet is no longer additive. Figure 2.6 illustrates this issue for a particular frame of the foreman sequence, in which the boundary matching technique is used for error concealment. In Fig. 2.6(a), the packet representing the 5^{th} row of MBs is the only packet received from the frame, and the rest of the MBs are concealed using that packet. In (b), the 6^{th} row is the only row received, and in (c), both the 5^{th} and 6^{th} rows are received. The darker pixels in each figure indicate higher gains in quality compared to not receiving any packets at all. Because of concealment of neighboring packets, the effect of receiving one packet extends beyond the immediate region represented by the packet. Therefore, adding the 6^{th} packet to the already transmitted 5^{th} packet does not provide an incrementally additive gain in quality corresponding to the gain that would occur if only the 6^{th} packet were received.

The solution, formulated in (2.2) and (2.3), takes into account the non-additivity of packet utilities by employing a myopic method for determining the packet orderings within the transmission queue. For each position in the transmission queue, the packet chosen is the one that provides the largest gain in quality after error concealment, given the packets that have already been added to the queue. Figure 2.7 shows an example user utility function obtained with the myopic packet ordering scheme. The error concealment causes the utility function to not be concave over the entire range. A result of this is that, when using a

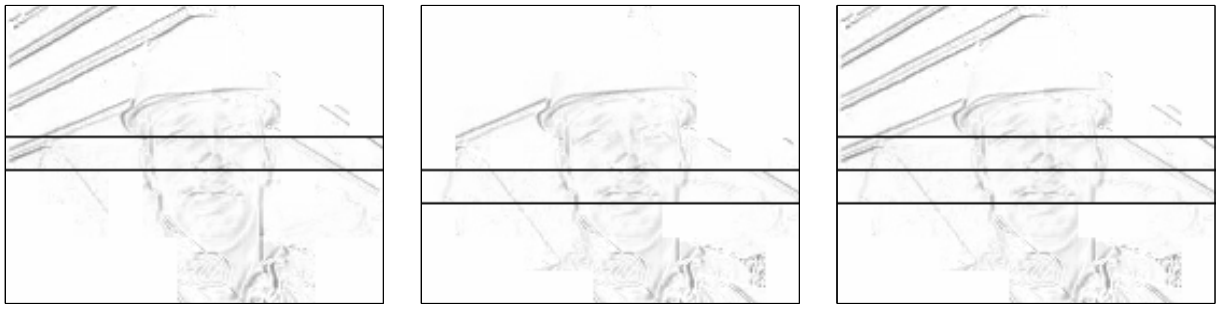

(a) MSE Gain = 262 (b) MSE Gain = 137 (c) MSE Gain = 272

Figure 2.6. Non-additive gain in quality due to complex concealment. Darker pixels indicate higher gain compared to not receiving any packets from the frame. The row borders are shown in black. (a) Packet containing MB row 5 received, (b) MB row 6 received, (c) MB rows 5 and 6 received (Total MSE gain significantly less than the sum of (a) and (b))

gradient-based scheduling scheme, a packet earlier in the transmission queue that provides a small reduction in distortion may receive a lower resource allocation, preventing a future packet that provides a greater reduction in distortion from being transmitted. To avoid this problem, for the complex concealment case, when determining the utility gradients to be used in (2.8), the actual gradient function is smoothed by calculating the gradient over multiple successive packets in the queue using,

$$u_{i,\pi_{i,k_i+1}}[k_i] = \frac{D_i[\Pi_i(k_i)] - D_i[\Pi_i(k_i+L)]}{\sum_{m=k_i+1}^{k_i+L} b_{i,\pi_{i,m}}}, \tag{2.18}$$

where L is the window length of successive packets over which the gradient is calculated. Figure 2.8, shows some simulation results using the same encoded sequences as in Sec. 2.5.1, and the same system parameters as in Table 2.1, where the performance due to using simple and complex concealment techniques is compared. In calculating the smoothed utility gradients as in (2.18), the window length is set to $L = 3$, which was empirically found to be

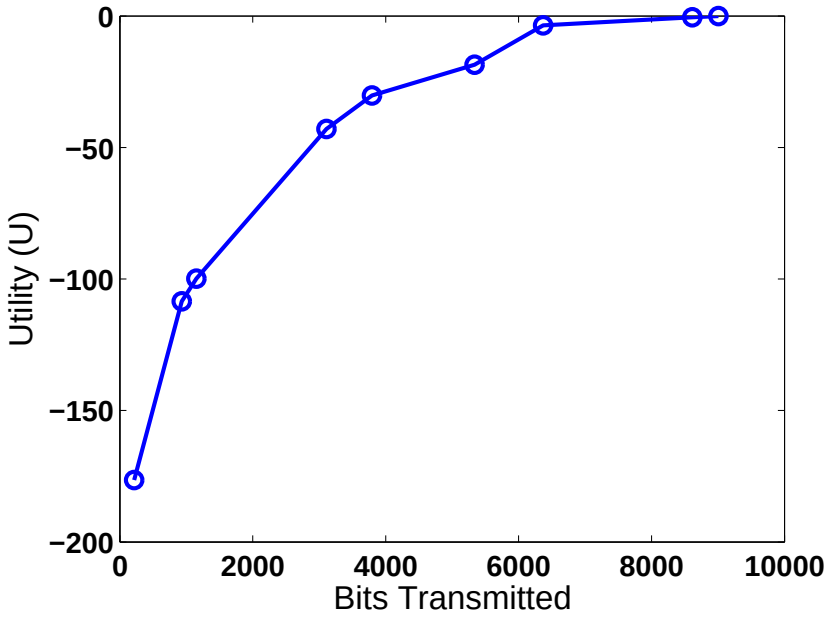

Figure 2.7. User utility function after packet ordering with myopic technique for complex concealment. The markers indicate bit boundaries for each packet.

an appropriate choice. The results are averaged over 100 frames and 5 channel realizations. The case in which the decoder uses a complex concealment technique but at the scheduler, a simple concealment technique is assumed during the packet ordering and resource allocation process, is also considered. When simple concealment is assumed, a video frame needs to be decoded only once in order to determine the utility gradients of each packet. When complex concealment is used, however, if there are no constraints on the dependencies allowed between packets, the video frame must be decoded M times, where M is the number of packets in the frame, to determine the concealment effect of each packet. Figure 2.8 shows that, although the packet ordering scheme with complex concealment is suboptimal, the performance of the system improves overall, as well as for most of the individual sequences. Not taking into account the decoder error concealment technique at the scheduler leads to a significant degradation in performance.

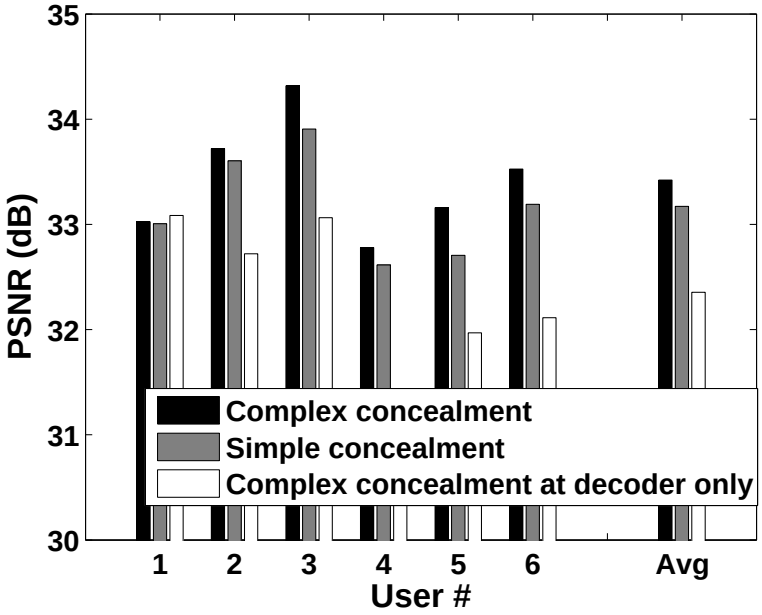

Figure 2.8. Performance comparison using simple and complex error concealment techniques at the decoder.

2.5.3. Offline or Simplified Packet Ordering Schemes

As temporal concealment, whether simple, or complex, uses information from previously decoded frames, the described packet ordering techniques require knowledge of the decoder state up to the previously transmitted frame. The decoder state at any time, however, is dependent on the specific channel realization up to that time, as well as the congestion in the network. Therefore, to achieve best results, the packet ordering must be done in real-time at the scheduler, which implies that the scheduler must be able to decode the video sequence given a specified set of packets, and determine the quality of the decoded video, in real-time.

Assuming that not all schedulers will have the necessary computational power to order the packets in real-time, this section illustrates a suboptimal technique for determining the packet ordering offline. An application of the technique, termed "Offline1" in Figs. 2.9 and 2.10, is to assume that the decoder state up to the previous packet group is perfect (i.e. all previous

packets are received without loss), when ordering the packets for the current group. A further extension of this method, termed "Offline2" is to assume that the decoder state up to all but the previous packet group is perfect, which assumes a first-order dependency among packet groups. In these methods, each packet can be stamped offline at the media server with an identifier marking its order within the packet group, as well as a utility gradient, which can be directly used by the scheduler. In the case of "Offline2", each packet will need to be marked with M different priority values where each value corresponds to the number of packets transmitted from the previous packet group. Figures 2.9 and 2.10 plot the performance of each system, real-time, Offline1, and Offline2, as the quality of the initially encoded sequence is increased. The content dependent schemes are also compared to the previously discussed content-independent queue length based scheme without packet ordering. Again, the system parameters in Table 2.1 are used. Figure 2.9 shows the average PSNR over all users and channel realizations and Fig. 2.10 shows the variance of PSNR across all users and channel realizations averaged over all frames of the sequence. As the initial quality increases, the bit rates of the sequences increase, leading to higher packet losses. As the number of packet losses increases, the gap between the real-time and offline methods also increases. When the initial quality is 34dB and 35dB, however, where the percentage of packets dropped per frame per user for the offline methods, is 10% and 16%, respectively, the performance of the offline methods remains close to that of the real-time scheme. This suggests that, if the video encoding is well matched to the channel, the offline schemes perform well but when mismatch occurs, the performance degrades. The offline packet prioritization schemes, however, still perform significantly better than queue dependent scheduling without packet prioritization. It must be noted that, although it performs slightly better, the "Offline2" method does not show a significant gain over simpler "Offline1" method.

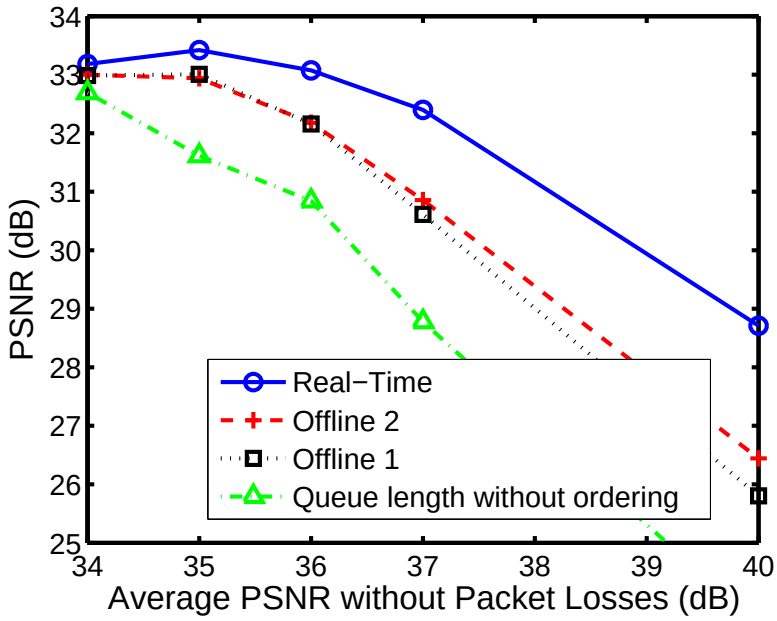

Figure 2.9. Comparison of average PSNR over all users and channel realizations with real-time ordering, content-dependent offline ordering and content-independent queue length based scheme. Higher initial quality leads to higher network congestion and more packet losses.

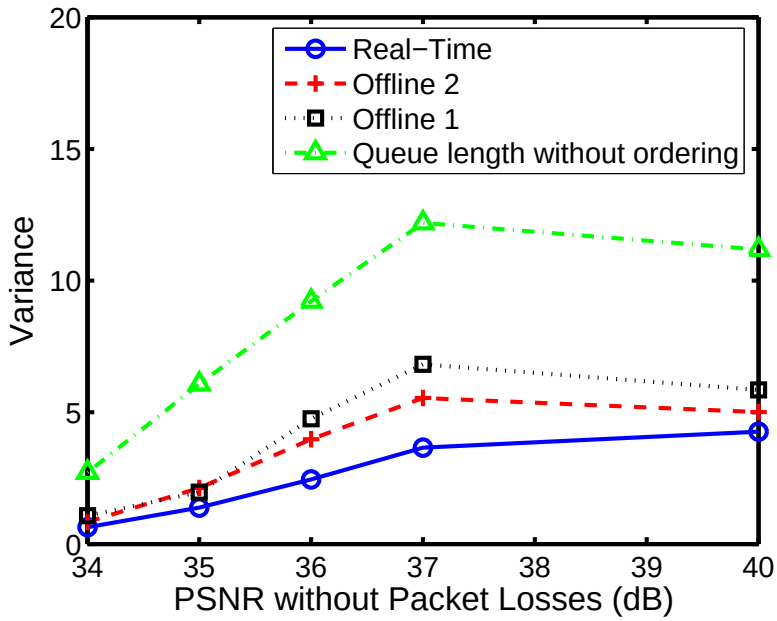

Figure 2.10. Variance of PSNR across all users and channel realizations

2.5.4. Error Resilient Video Encoding

When scheduling and transmitting pre-encoded video packets over wireless channels, some packets are inevitably dropped due to inadequate channel resources. Error resilient video encoding schemes alleviate the ill-effects of packet loss on the decoded video [**6**]. Error robust video compression, however, involves a trade-off with greater robustness leading to lower compression efficiency. Therefore, the performance of specific error resilience tools and compression schemes must be analyzed under realistic channel conditions. This section examines some of the trade-offs important to this work.

Among the tools that trade-off compression efficiency for error resilience are the slice structure, which allows for resynchronization within a frame, flexible macroblock ordering, which enables better error concealment, and constrained intra prediction as well as random I MB insertion, which reduce error propagation. This work assumes a slice structure consisting of one row of MBs per slice, which achieves a reasonable compromise between error robustness and compression efficiency.

Table 2.2, shows the trade-off between error resilience and compression efficiency due to random I MB insertion. The system parameters are kept the same as in the previous simulations and the performance results are shown for the foreman sequence given that each of the six sequences is initially encoded using the given numbers of random I MBs per frame. The quality of the encoded sequence without packet losses is maintained close to 35dB through rate control. As the number of random I MBs increases, the bit rate of the encoded stream increases, which leads to higher packet drop rates at the scheduler and resultant loss in video quality. Not using I MBs also degrades the video quality by increasing error propagation. Similarly, Figs. 2.11 and 2.12 shows a comparison between sequences encoded using intra pre-

Table 2.2. Trade-off between error resilience and compression efficiency due to random I MB insertion

Random I MBs	Input Rate (kbps)	Pct Pkts Dropped	Received Avg PSNR(dB)	PSNR Loss
0	153	1.0	32.7	2.8
2	153	0.4	33.4	1.6
4	**176**	**0.8**	**34.3**	**0.9**
6	200	1.6	34.1	1.4
8	200	2.1	33.6	1.4
10	200	2.8	33.2	1.4
12	248	5.1	32.6	2.8

diction, a technique proposed in H.264 to increase compression efficiency, and those encoded using constrained intra prediction. In intra prediction, intra MBs are predictively dependent on neighboring MBs, some of which may be inter, of the same slice. In a packet lossy system, such dependencies lead to error propagation. Constrained intra prediction limits intra prediction to using only the neighboring intra MBs, which eliminates error propagation at the cost of lower compression efficiency. Figure 2.11 shows a comparison between the average PSNR of each users received sequence with and without constrained intra prediction. Figure 2.12 shows the difference in encoded bitrate for each scheme. From Figs. 2.11 and 2.12, it is apparent that the gain in compression efficiency due to intra prediction is not sufficient to offset the performance loss due to error propagation. A relationship between the source encoding rate and the quality of the received video can also be determined. Given similar channel conditions, lower source rates lead to lower packet losses at the cost of higher distortion due to compression artifacts. On the other hand, higher source rates can lead to lower compression artifacts, at the expense of higher packet losses, some of which can be concealed.

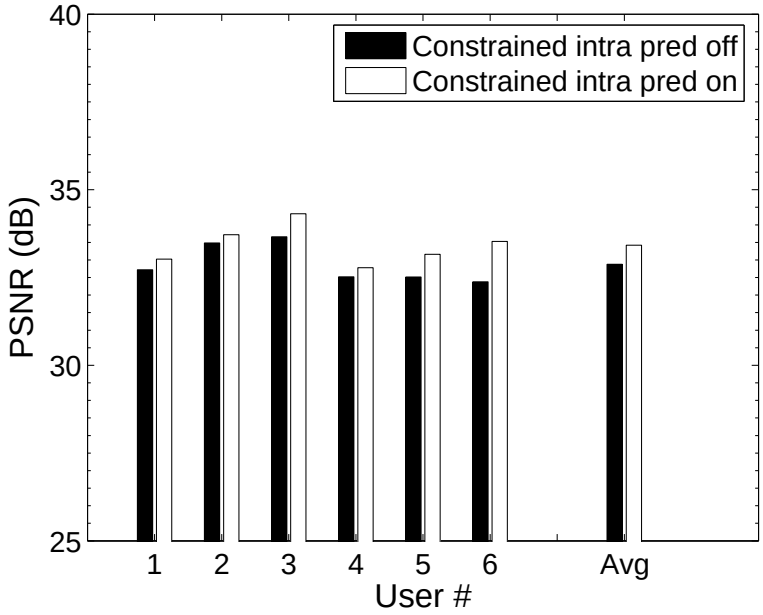

Figure 2.11. PSNR of received video if original video is encoded with and without constrained intra prediction. Average quality without packet losses for all sequences is close to 35dB.

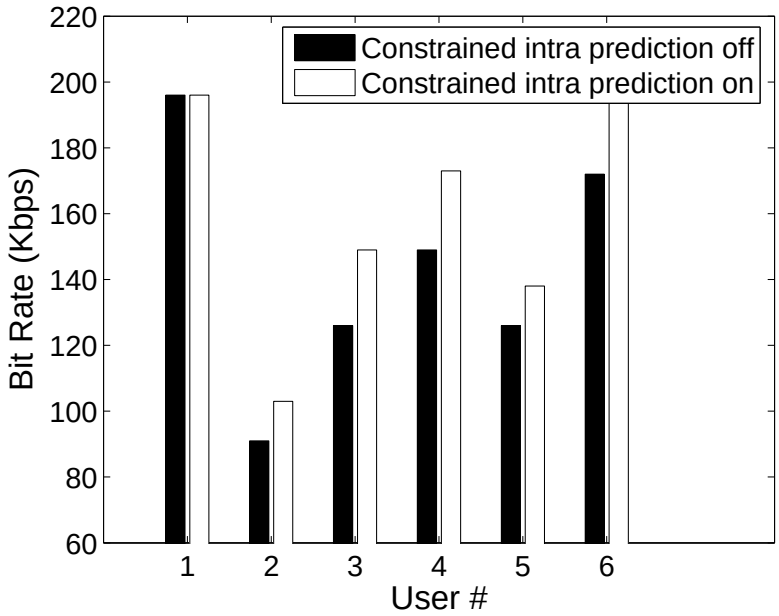

Figure 2.12. Encoded bitrate of original video with and without constrained intra prediction.

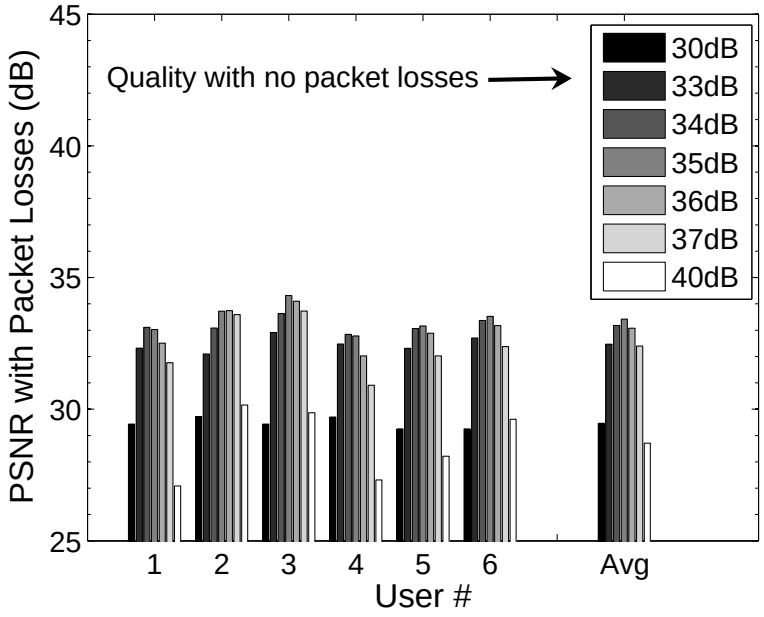

Figure 2.13. PSNR of received video with varying initial bit rates corresponding to varying quality prior to transmission losses.

Channel simulations with varying source encoding rates can determine the optimal encoding rates under the given average channel conditions. Figure 2.13 shows the performance results for a multiple user system where each user's sequence is initially encoded such that the decoded quality without packet losses is close to the specified average PSNR. Then, the decoded PSNR is measured after packets are dropped at the transmission queue using the packet scheduling scheme. Figure 2.13 shows that, given the average channel conditions, an appropriate source rate for the pre-encoded video sequences can be found. Therefore, the media server can potentially keep multiple source bit streams at different rates for each video sequence and choose the appropriate stream based on the average channel conditions.

2.6. Conclusions

This chapter demonstrates that a resource allocation scheme that maximizes a weighted sum of the rates assigned to each user where the weights are determined by distortion-based utility gradients, is a simple but effective solution for downlink packet scheduling in wireless video streaming applications. It provides an optimal solution for the case when the video packets are independently decodable and a simple error concealment scheme is used at the decoder. It is also shown that with complex error concealment at the decoder, a suboptimal myopic solution with appropriately calculated distortion utility gradients can still provide excellent results. The system depends on the compression and error resilience schemes used at the encoder.

CHAPTER 3

Scalable Video Encoding

This chapter discusses the application of the content-aware resource allocation formulation in a scalable video coding framework. The chapter presents some of the natural advantages to be had, and some pitfalls to be avoided, when using scalable coded video in conjunction with a content-dependent gradient-based scheduling policy.

3.1. Overview of Scalable Video Coding

An overview of the techniques and applications of scalable video coding, especially as it pertains to SVC [**61**], the emerging scalable extension to H.264/AVC [**30**], is provided in [**35, 37**]. In general, a scalable video bitstream offers three different categories of scalability that may be used individually, or in combination. They are: spatial scalability, which allows the transmission of the same video sequence at different resolutions depending on the user requirements or bandwidth constraints, temporal scalability, which allows the transmission of the video sequence at different frame rates without error propagation due to the skipped frames, and quality (SNR) scalability, which allows the transmission of progressively refined bitstreams depending on the available data rates. This work, focuses on optimizing over temporal and SNR scalability levels and excludes spatial scalability since it is reasonable to assume that the spatial resolution will remain static within one video streaming session.

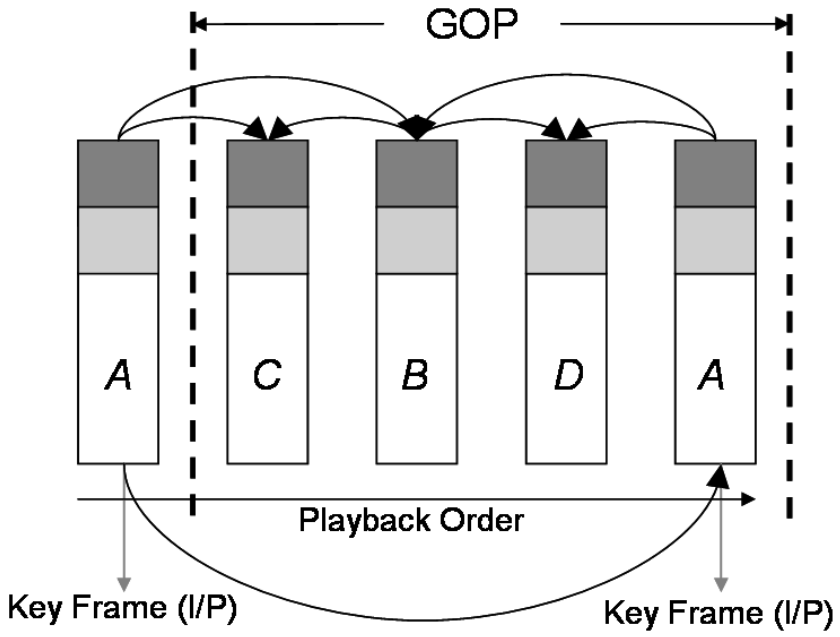

Figure 3.1. Structure of scalable coded bitstream

Figure 3.1 shows a group of pictures (GOP) in the typical structure of a scalable coded bitstream, in which hierarchical bi-prediction is used for temporal scalability, and fine granularity scalability (FGS) is used for progressive refinement of quality. The shaded part of each frame denotes an additional progressive refinement (PR) layer. While the playback order of the GOP is as shown, the decoding order is determined by the dependencies due to motion prediction, and will be the frames denoted A, B, C, and D, in that order, where frames denoted B, C, and D are bi-predictive (B) frames. Hierarchical bi-prediction makes use of the ability provided in recent video coding standards, such as H.264/AVC, to use B (bi-predictive) frames as references for other B frames. The hierarchical prediction scheme is illustrated in Fig. 3.1 by the arrows depicting the motion prediction directions for each

picture. The scheme allows for a hierarchy of B frames such that frames not used as references for motion compensation can be discarded from the bitstream with a corresponding loss in temporal resolution but with no error propagation across multiple GOPs [**61**].

Quality scalability can be achieved in the bitstream by encoding progressive refinement layers in which the transform coefficients of macroblocks are encoded at progressively finer resolution (smaller quantization step sizes). The resulting quantization levels are then bit-plane coded to obtain fine grained scalability layers. Further details on fine granularity scalability can be found in [**38, 39**].

As shown in Fig. 3.1, the scalable coded bitstream with hierarchical bi-prediction and progressive refinement can be setup such that a key frame, which is an I (Intra) or P (Inter) frame of the sequence, is predictively dependent only on the base layer of the previous key frame. For the sake of compression efficiency, however, non-key frames, which do not contribute to error propagation over multiple GOPs, can use the highest rate points (i.e., decoded frames with enhancement layers) of their reference frames for motion compensation. It must be noted that another approach is to encode all frames in the sequence such that they are only dependent on each other's base layers for motion compensation. At the cost of lower compression efficiency, such an approach will ensure that no error propagation occurs as long as the base layers of all pictures are received.

This work assumes that each application layer packet contained in the media server is independently decodable as specified in the Network Abstraction Layer (NAL) unit structure provided by H.264 [**61, 62**]. Typically, a NAL unit would consist of one layer (base or PR) of a coded frame. For transport from the media server to the base station, each coded NAL unit is packeted into one or more RTP packets but it is reasonable to assume that no two NAL units will be contained in one RTP packet. Therefore, each video packet will contain

information about its own decoding deadline, in addition to the number of bits contained in the packet. It can also be assumed that the transport packets will be further fragmented into smaller packets at the MAC layer prior to transmission over the air interface. In order for a tractable media-aware scheduling scheme to be implemented at the base station, each packet will need to contain a media-aware scheduling metric (described later) that can potentially be calculated offline.

The decoding deadline of a packet stems from the video streaming requirement that all the packets needed to decode a frame of the video sequence must be received at the decoder buffer prior to the playback time of that frame. As in Sec. 2.1 multiple packets (e.g., all the packets belonging to one GOP) can have the same decoding deadline. Any packet that is left in the transmission queue after its decoding deadline has expired must be dropped since it has lost its value to the decoder. Note that the true decoding deadlines for different packets within the same GOP may be different depending on the decoding order of the packets as well as the temporal order in which the frames are played back.

In a scalable progressively coded bitstream the base layer of a particular frame must be received at the decoder in order for the information from subsequent progressive refinement layers to be correctly retrieved. Therefore, scalable video compression provides some intrinsic constraints on the ordering of packets, which must be taken into account in the packet scheduling schemes at the scheduler. If the entire base layer of a frame is not received, then that frame is assumed lost and the loss is concealed by copying the previously decoded frame, thus reducing the temporal resolution of the sequence. A PR layer, however, can be partially received and decoded and, in this work, no error concealment is performed on partially received PR layers. More complex error concealment techniques that involve interpolating from neighboring received frames are also possible and can potentially be included within this

framework but are not numerically investigated here. Again, as in 2, the error concealment technique employed at the decoder has an impact on the quality of the received video, and therefore, must be taken into account when determining the importance of video packets.

3.2. Packet Scheduling with SVC

The most important aspect of this work is that of choosing a packet scheduling strategy and a content-aware utility metric to be used within the gradient-based scheduling framework discussed in Chapter 2. In doing so, special attention needs to be paid to the natural advantages and potential pitfalls of using a scalable video coding scheme. As stated in Sec. 2.2, the key idea in the proposed technique is to sort the packets in the transmission buffer for each user based on the contribution of each packet to the overall video quality, and then, to construct a utility function so that the gradient of the utility reflects the contribution of each packet. A key feature that adds to the tractability of the framework is that the scheduling in a given time slot is performed based only on the information available at the start of that time slot and is not dependent on looking ahead at future states of the system. Scalable video coding, and especially, fine granularity scalability, can be a useful tool to employ within this framework.

In gradient-based scheduling algorithms users receiving packets with a larger first-order change in utility are given priority. Therefore, the ordering strategy used for generating the packet ordering, Π_i, for each user, i, has an impact on the priority assigned to that user in the resource allocation scheme. Also, if sufficient resources are not available to transmit all the packets in the queue, the packet ordering strategy will determine which packets will be dropped from the transmission queue of a user. Scalable video coding offers a natural packet order that constrains the possible packet scheduling policies at the scheduler. The problem

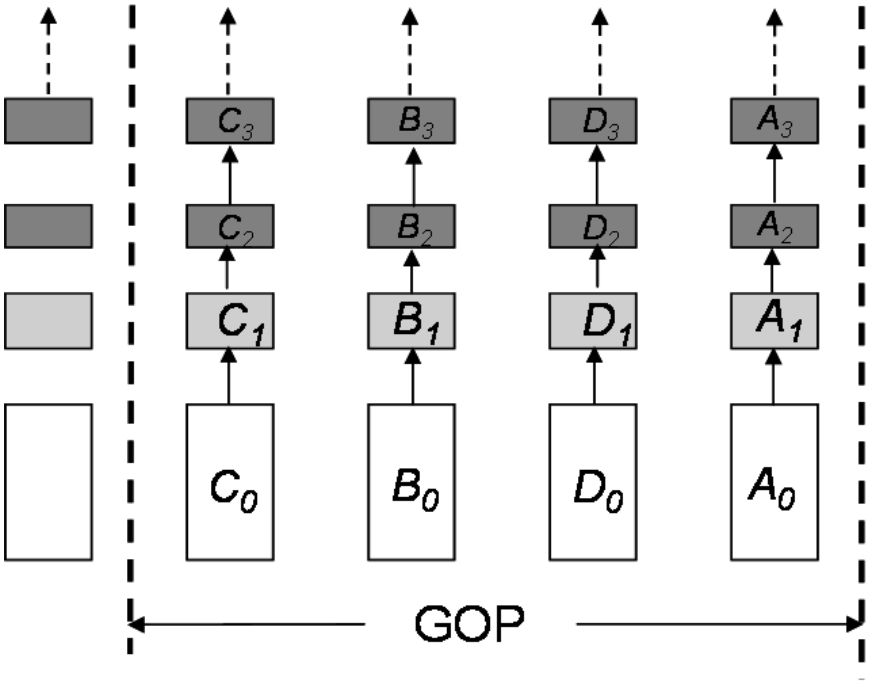

Figure 3.2. Scalable coded bitstream with PR layers fragmented into multiple packets.

then becomes one of adhering to the intrinsic ordering constraints but still choosing a packet ordering policy that will improve the performance of a gradient-based scheduling scheme. This work considers a few different ordering methods described below.

3.2.1. Ordering Method I- Quality First

This is the same as that discussed in [**54**] in which the PR packet fragments and base layer of the highest temporal level of the GOP are dropped first in that order. For example, if the packet fragments of each frame are labeled as in Fig. 3.2 for a GOP size of 4 (with the motion prediction dependencies as shown in Fig. 3.1), the ordered set, Π_i at the beginning of transmission for the GOP would be $\Pi_i = \{A_0, A_1, ..., B_0, B_1, ..., C_0, C_1, ..., D_0, D_1, ...\}$ in order of transmission. Note that it is assumed that each PR layer is further subdivided into smaller fragments. This method sacrifices temporal resolution in order to maximize the

quality of each transmitted video frame. Figure 3.3 shows the distortion as a function of transmitted bits using Method I for a particular GOP of the "*carphone*" sequence. It is clear from Fig. 3.3 that the utility function derived from this ordering technique is not conducive to a gradient-based scheduling technique as it will not be concave. The sudden reduction in distortion occurs when an additional base layer picture is transmitted, resulting in an increase in temporal resolution of the GOP.

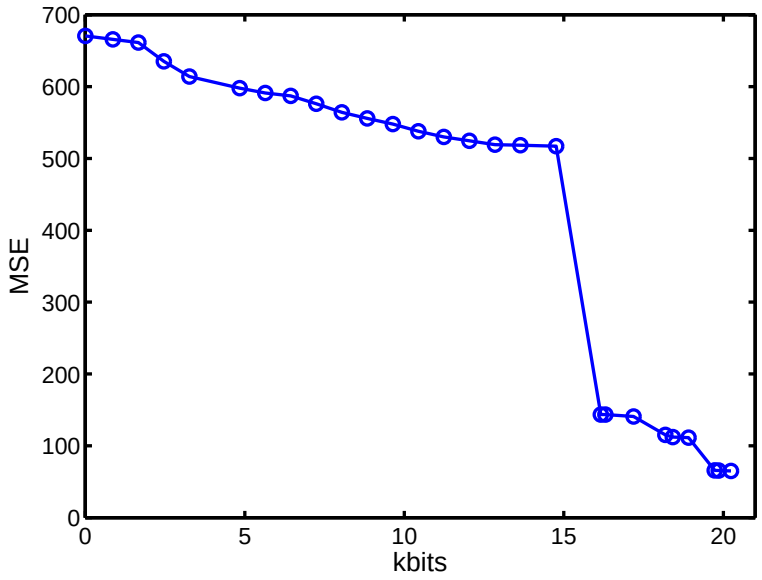

Figure 3.3. Distortion-bits curve for one GOP in carphone sequence using Method I.

3.2.2. Ordering Method II- Temporal First

The PR packets of the highest temporal level are dropped first, and after all PR packets in the GOP have been dropped, the base layer of the highest temporal level is dropped. Again, assuming the GOP structure in Figure 3.2, this would imply that Π_i would be $\{A_0, B_0, C_0, D_0, A_1, A_2, ..., B_1, B_2, ..., C_1, C_2, ..., D_1, D_2, ...\}$. Method II maintains temporal

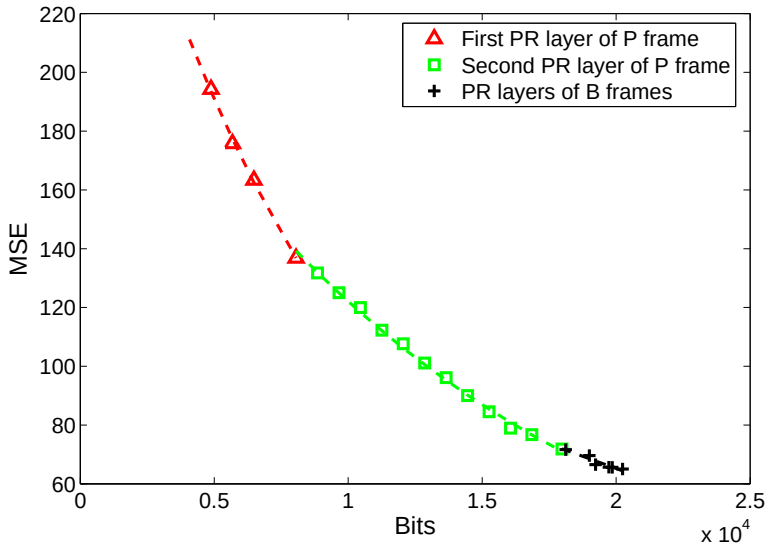

Figure 3.4. Approximation of the distortion-bits curve for one GOP in carphone sequence using Method II.

resolution at the cost of individual image quality by giving the highest priority to the base layer packets of the entire GOP. This reduces the "jerkiness" of the decoded video.

Figure 3.4 shows a typical distortion-bits curve for the PR packet fragments of a GOP taken from the *carphone* sequence using method II. The markers indicate packet fragment boundaries. The dotted line shows an exponential approximation of the distortion-bits curve of the form, $\beta_{k_i} e^{\alpha_{k_i} R}$, where R is the number of bits for each key frame PR packet, and a linear approximation of the curve for the non-key frame PR packets. Similar behavior can be observed for the PR packets of other sequences as well. This approximation enables the scheduler to calculate the utility gradients of PR packet fragments at the MAC level, using only the constants β_{k_i} and α_{k_i}, which can be signaled with the larger transport packets from the media server.

3.2.3. Ordering Method III- Hybrid

The base layer of the key picture is given the highest priority. Subsequent packets are ordered such that the next highest priority is given to the decodable packet (decodable given only the higher priority packets are received) that provides the largest reduction in distortion per bit given that it is received at the client. Figure 3.5 shows an example of Method III in which the packet labels are the same as in Fig. 3.2. At the first step, only the base layer packet of the key frame, A_0 is decodable. If A_0 is decoded, then both B_0 and A_1 are decodable and the packet with the largest utility gradient is picked. Once that packet, in this case B_0, is added to the queue, the set of new decodable packets is A_1, B_1 and C_0. Method III is the most flexible strategy but is more complex to implement and results show little gain compared to Method II.

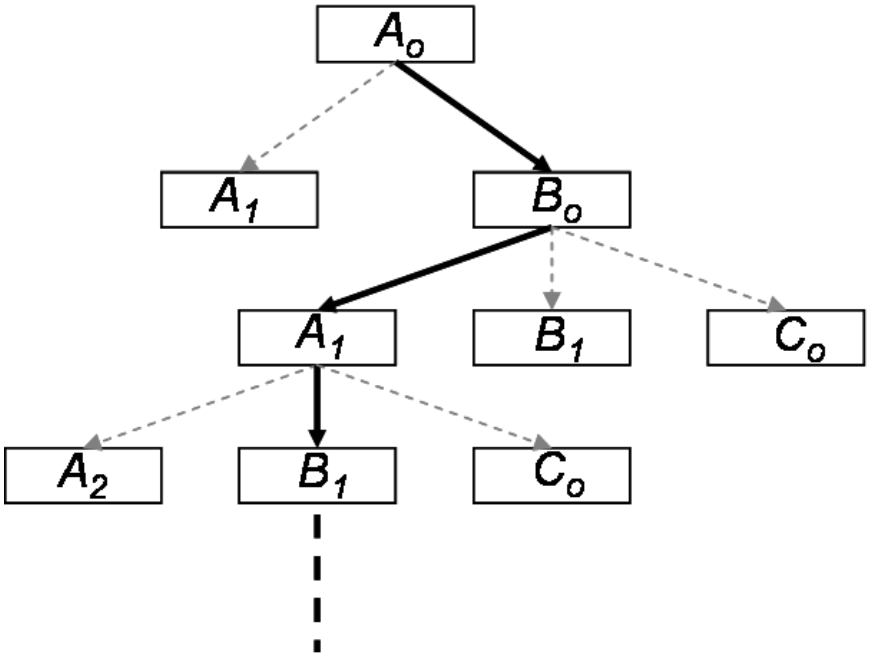

Figure 3.5. Packet ordering using Method III.

3.3. Simulations

Simulations were performed to determine the gains to be expected by using the gradient-based scheduling framework for content and channel dependent scheduling of scalable video. The same sequences as in Chapter 2 were used in the simulations. The sequences were encoded with hierarchical bi-prediction and fine granularity scalability slices using the JSVM reference software for the SVC extension to H.264 [**63**]. The GOP size was set at 4 for all the experiments with the key picture in each GOP, except the first, set to be a P frame. The transmission time per GOP was set at 128 msec. The sequences were encoded such that at the highest rate, and with no losses, they had a decoded Y-PSNR of approximately 35dB. A sufficient buffer time was assumed to be available for the reliable transmission of the first frame (I frame) of each user. If a video packet could not be completely transmitted within a given transmission opportunity, it was fragmented at the MAC layer. As mentioned in Sec.3.1, the base layer packet must be completely received in order to be useful but the PR packets may be partially received and still be decoded. The simple decoder error concealment technique mentioned in Sec.3.1 is used to conceal losses due to dropped packets.

The wireless system parameters were set to be the same as in the simulations in Chapter 2, as specified in Table 2.1. The average PSNR results are the average Y-PSNR over 100 frames of each sequence under 5 different channel realizations. The variance of PSNR across users is calculated at each frame, over 5 different channel realizations and the six users, and then averaged over the 100 frames.

3.3.1. Comparison of Packet Ordering Methods

Table 3.1 shows a comparison in performance between the different ordering methods discussed in Sec. 3.2. Modified Method II indicates the Method II ordering scheme where the exponential approximation is used to calculate the distortion-based utility gradient. The number of PR layers is set to 2 for each encoded sequence with the PR packet fragments set at size 100 bytes. It can be seen that Method I shows the worst performance while the other methods show similar performance both in terms of average and variance of received PSNR. Method II with the exponential approximation has the smallest average PSNR and smallest variance across users. It must be noted that the packet ordering scheme in Method II is significantly simpler than that of Method III. The better performance of the exponential approximation for Method II can be attributed to the smoothing of the utility functions, which makes them more amenable to the gradient-based resource allocation framework.

Table 3.1. Comparison of Ordering Methods (Total Power: $P = 2.5$W)

	Avg PSNR (dB)	Var of PSNR
Method I	25.72	44.21
Method II	30.99	2.40
Method III	31.05	2.16
Modified Method II	31.12	2.01

3.3.2. Comparison with Content-Independent Metric

The proposed content-aware scheme was compared with a content-independent maximum throughput scheduling scheme as in [**54**]. Maximum throughput scheduling was achieved by letting the utility gradients in (2.10), u_i, equal 1 for all users with non-empty transmission

queues. Figure 3.6 shows a comparison of the average received PSNR between the distortion-based scheduling metric and maximum throughput scheduling over varying total power, and therefore, varying network operating conditions. Method II is used for packet prioritization in both schemes and the calculation of the distortion-based utility metric is performed using the exponential approximation in the modified Method II. Cases when the bitstreams were encoded to contain 1, 2, and 3 PR layers are considered. Figure 3.6 shows that the distortion-based metric performs better in terms of average received PSNR over the tested range of operating conditions. As should be expected, Fig. 3.7, which depicts the variance across users and channel realizations using both schemes, shows that in a maximum throughput scheduling scheme, which does not guarantee fairness across users, the variance of PSNR across users is high.

Figure 3.6 also shows a lower average received PSNR at higher powers when more PR layers are used for each sequence. When more PR layers are used, the overall quality of each frame is kept fixed, and as a result the quality of the base layer is reduced with a corresponding reduction in size of the base layer. This provides greater flexibility to adapt to degraded channel conditions but comes at a cost of larger PR layers where the incremental gain in quality per bit may be lower.

For a more fair comparison of the proposed scheme with a reasonable content independent scheme, a similar gradient-based scheduling framework but with a queue length dependent metric as in the M-LWDF (Modified-Largest Weighted Delay First) algorithm proposed in [**24**] is also compared. In this case, the utility gradient, u_i, in (2.10), is replaced by the total length in bits of the remaining packets in user i's transmission queue. Figures 3.8 and 3.9 show comparisons in terms of average received PSNR and variance of PSNR between the content dependent and queue-length dependent schemes over varying total power. Again,

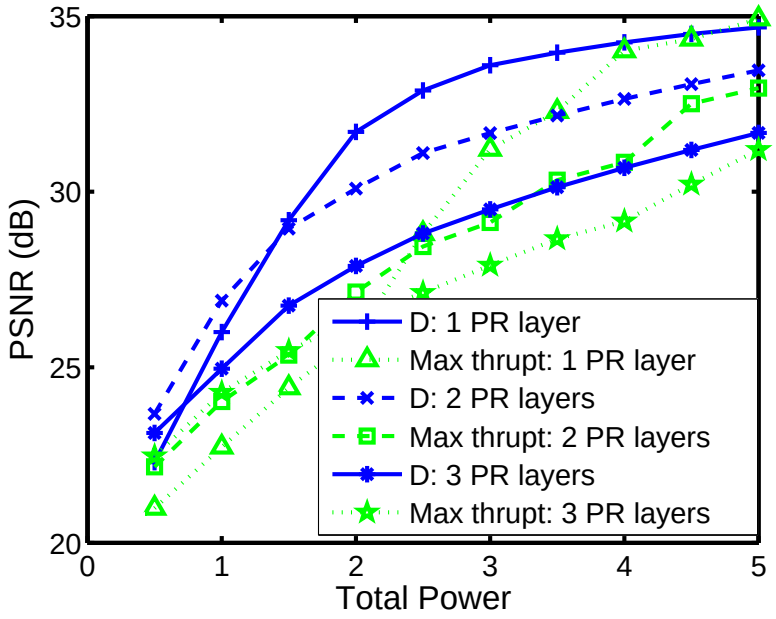

Figure 3.6. Comparison of average PSNR between distortion gradient based and maximum throughput scheduling

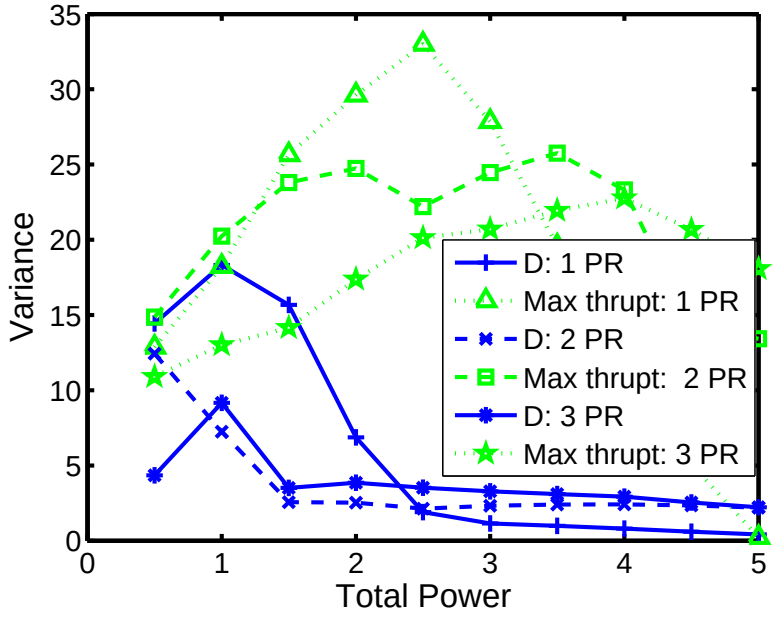

Figure 3.7. Comparison of variance across users and channel realizations between distortion gradient based and maximum throughput scheduling

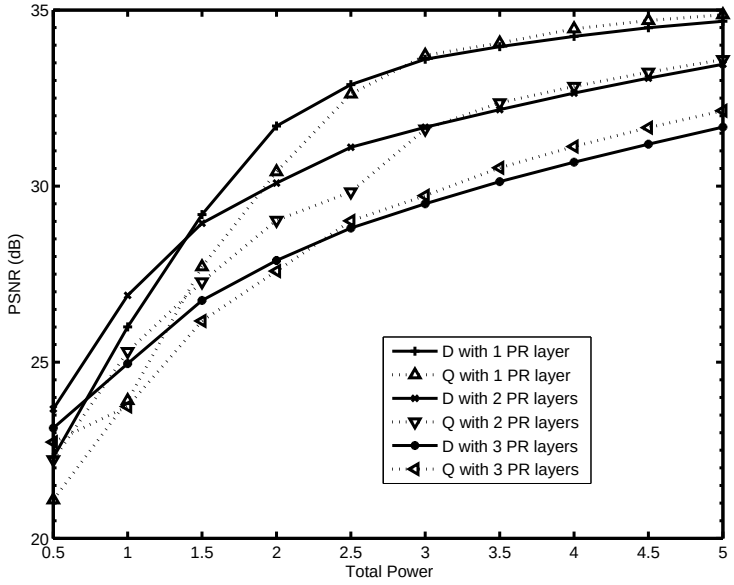

Figure 3.8. Comparison of average received PSNR between distortion gradient based metric and queue dependent metric; (D: Distortion-based metric, Q: Queue length-based metric)

Method II is used for packet prioritization in both schemes and modified Method II is used for calculation of the distortion-based utility metric. Figure 3.8 shows that the distortion-based metric performs better over a wider range of operating conditions, and that as the achievable data rates are reduced due to limitations on resources, the degradation in quality is more graceful than that of the queue length based metric. As shown in Fig. 3.9, the variation in quality across users is also more significant for the queue-length dependent metric, especially at low total power.

3.3.3. Comparison with H.264/AVC

The proposed scheme using SVC was also compared to the corresponding scheme using H.264/AVC, which is discussed in [**64**]. As in [**64**], the packets belonging to each key frame

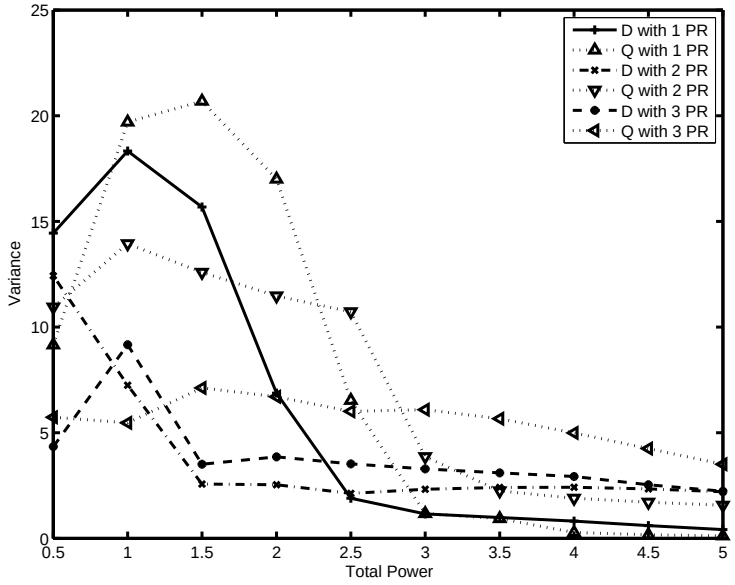

Figure 3.9. Comparison of variance of PSNR between distortion gradient based metric and queue dependent metric.

in the H.264/AVC coded bitstream were divided into multiple slices where each slice corresponded to one row of macroblocks. For compression efficiency, the non-key (B) frame packets which are significantly smaller in length are not divided into multiple slices. As in the case of SVC, the AVC sequences were encoded such that, with no losses, they had a given decoded Y-PSNR. In order to compare with AVC at different bit rates, the results were compared where the decoded Y-PSNR without losses of the AVC bitstream was set at 33dB, 34dB, and 35dB. The packet ordering and resource allocation was performed as described in [**64**], with the transmission queue consisting of one GOP of size 4, which includes 9 packets for the key frame (P) and 3 packets containing B frames. Figures 3.10 and 3.11 show comparisons in performance between SVC and H.264/AVC under the same network conditions. It can be seen that due to its adaptability to the channel conditions, scalable video coding offers a significant improvement in performance over conventional H.264/AVC

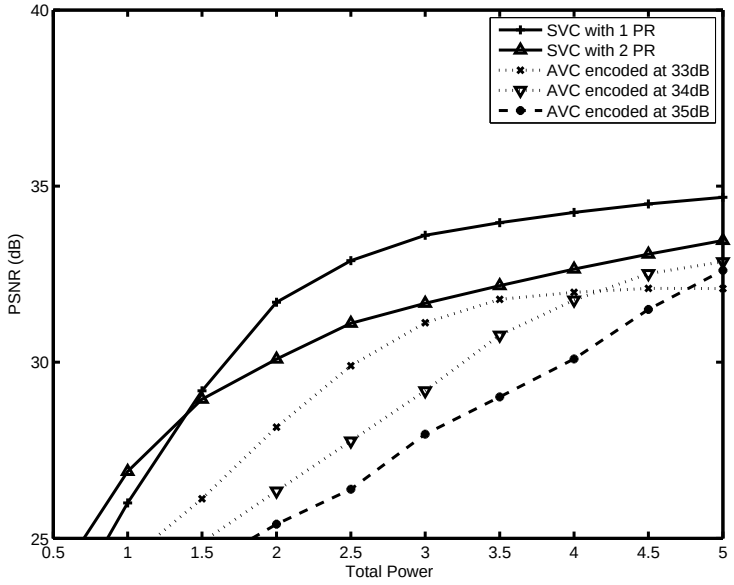

Figure 3.10. Comparison of average received PSNR between scalable coded video and H.264/AVC coded video.

in a wide operating range. The improvement in performance of SVC can be attributed to its resilience to error propagation due to dropped packets, as well as the finer granularity of quality that is possible through the use of FGS layers. The higher PSNR variance of SVC at lower powers seen in Fig. 3.11 can be attributed to the loss of entire base layer packets, which leads to loss of temporal resolution. The SVC coded streams, however, show a higher average PSNR and lower variance of PSNR over a larger range of conditions, when compared to AVC.

3.4. Conclusions

This chapter presents a content-aware packet scheduling and resource allocation scheme for use in a scalable video coding framework that achieves a significant improvement in performance over content independent schemes. Simulation results show that the proposed

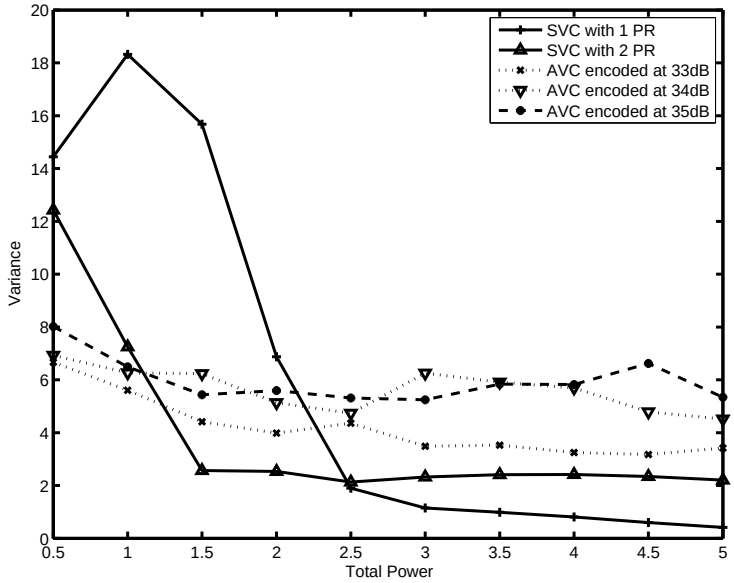

Figure 3.11. Comparison of variance of received PSNR between scalable coded video and H.264/AVC coded video

content-aware metric provides a more robust method to allocate resources in a downlink video transmission system. It is also apparent that scalable video coding offers the possibility of using simple packet prioritization strategies without compromising the performance of the system. The packet prioritization can be performed offline and signaled to the scheduler along with the utility metrics of each packet. Most importantly, significant gains in performance can be seen in using scalable video coding as opposed to conventional non-scalable video coding over the types of time-varying networks studied in this work.

CHAPTER 4

Resource Allocation in Packet Lossy Channels

Previous chapters assume the availability of perfect channel state information at the scheduler prior to making a scheduling decision. As a result, they use a zero-outage capacity model to determine the achievable data rates for each user. Therefore, the losses considered in the previous simulations occur only when packets are not transmitted on time due to a combination of the congestion at the transmission queue, and the scheduling priority of each packet. This chapter considers a realistic scenario in which only an imperfect estimate of the channel state is available. In this case, an outage capacity model can be used to determine a probability of channel loss based on the estimated channel state, the allocated resources, and the transmission rate [**65**]. Random channel losses combined with complex error concealment at the decoder make it impossible for the scheduler to obtain a deterministic estimate of the actual distortion of the sequence at the receiver. Instead, the scheduler must use the expected quality at the receiver in order to determine its scheduling decisions. Efficient methods exist for recursively calculating the expected distortion at the receiver [**8, 66**]. This chapter uses a scheme for ordering the packets by their contribution towards reducing the expected distortion of the received video to jointly optimize the resource allocation (power and bandwidth) and transmission rates assigned to each user such that the expected distortion over all users is minimized.

4.1. Packet Ordering with Expected Distortion

Three factors that affect the end-to-end distortion of the video sequence are, the source behavior (quantization and packetization), the channel characteristics, and the receiver behavior (error concealment) [**67, 6**]. For the purposes of this work, the source is assumed to be pre-encoded and packeted. There is flexibility, however, in determining the ordering of source packets such that the most important packets have a greater likelihood of being received at the decoder. Using an outage capacity model, the probability of loss of each transmitted packet can be estimated based on the imperfect channel state information available at the scheduler. As in previous chapters, the error concealment technique employed at the decoder is assumed to be known by the scheduler. The rest of this section describes a method for ordering the video packets within each user based on the contribution of the packets towards reducing the expected distortion of the sequence. Since the same technique is used for all users, the user index, i, is omitted during this discussion.

4.1.1. Expected Distortion Calculation

For the purposes of this work, a complex error concealment technique is assumed that estimates the motion vector of a lost macroblock to be the median motion vector of the macroblocks immediately above it, if they are received. If the top macroblocks are also lost, then a zero motion vector is assumed leading to the copying of pixel values from the co-located macroblock in the previous frame. Given that the video frame is divided into slices where each slice is a row of macroblocks, this assures that each slice is only dependent on the previous frame, and its top neighbor in the current frame for error concealment. In that

case, the expected distortion of the m^{th} packet/slice can be calculated at the encoder as,

$$\begin{aligned} E[D_m] &= (1-\epsilon_m)E[D_{R,m}] + \epsilon_m(1-\epsilon_{m-1})E[D_{LR,m}] \\ &\quad +\epsilon_m\epsilon_{m-1}E[D_{LL,m}], \end{aligned} \tag{4.1}$$

where ϵ_m is the loss probability for the m^{th} packet, $E[D_{R,m}]$ is the expected distortion if the m^{th} packet is received, and $E[D_{LR,m}]$ and $E[D_{LL,m}]$ are respectively the expected distortion of the lost m^{th} packet after concealment when packet $(m-1)$ is received or lost. The distortion can be efficiently calculated using a per pixel recursive algorithm called ROPE, which was originally proposed in [**8**], and modified for the case of sub-pixel interpolation in [**66**].

Assuming an additive distortion measure, the expected distortion of a frame of M packets, denoted ED, can be written as,

$$ED = \sum_{m=1}^{M} E[D_m]. \tag{4.2}$$

4.1.2. Packet Ordering

Let $\mu_m \in \{0,1\}$ denote whether packet m is transmitted ($\mu_m = 1$), or not ($\mu_m = 0$), during the current transmission time-slot. Then, a Lagrangian cost function can be written to express the problem of determining the transmission policy vector, $\mu = \mu_1, \mu_2, ..., \mu_M$, that minimizes the expected distortion of the frame given a limited bit budget as,

$$\mathcal{L}(\boldsymbol{\mu}, \boldsymbol{\epsilon}; \lambda) = \sum_{m=1}^{M} E[D_m(\mu_m, \epsilon_m, \mu_{m-1}, \epsilon_{m-1})] + \lambda b(\mu_m), \tag{4.3}$$

where $\epsilon = (\epsilon_1, \epsilon_2, ..., \epsilon_M)$ denotes the vector of packet loss probabilities, ϵ_m, of each packet m, and λ is a real parameter determining the transmission cost. $b_m(\mu_m)$ denotes the number of bits transmitted from packet m, which will be 0, if $\mu_m = 0$, and the length of the packet, if $\mu_m = 1$.

For a fixed ϵ, let the mode vector μ^* be the one that minimizes the cost function, i.e.,

$$\mu^*(\lambda, \boldsymbol{\epsilon}) = \arg \min_{\mu \in \{0,1\}^M} \mathcal{L}(\mu, \epsilon; \lambda). \tag{4.4}$$

Given the error concealment technique discussed above which limits the dependencies between packets, the above optimization can be performed efficiently using a dynamic programming technique.

Now, increasing the value of λ corresponds to increasing the cost of transmitting each packet, and as a result, leads to decreasing the number of transmitted packets in μ^*. Therefore, there exists some λ_{max} such that $\mu^*_m = 0$ for all m, and assuming that all packets have some contribution towards reducing the expected distortion, there exists some λ_{min} such that $\mu^*_m = 1$ for all m. The threshold, λ_m at which the mode of each packet m switches from $\mu^*_m = 0$ to $\mu^*_m = 1$ determines the order in which each packet is added to the transmission queue (i.e., packets with larger values of λ_m correspond to more important packets in terms of reducing the expected distortion). Note that the thresholds depend on the probability of loss, ϵ, as well, and cannot be known *a priori*.

4.2. Resource Allocation

As in Chapters 2 and 3, the available resources are the total transmission power, and the bandwidth (represented by the number of available spreading codes). Therefore, the resource allocation consists of determining the appropriate transmission power, p_i, and number of

spreading codes, n_i for each user i, at each transmission time-slot. In the previous chapters, however, the exact channel state at that time-slot is assumed to be known, and therefore, given a p_i and n_i allocation, the achievable error-free transmission rate, r_i, can be precisely calculated. In the case, when the exact channel state is not known, and only an estimate of the channel state is available, it is also necessary to consider the probability of loss in the channel due to random channel fading that may occur during the transmission. Depending on the assumed wireless channel model, the probability of loss can be calculated, using an outage probability formulation [**65**], as a function of the assigned transmission power, bandwidth, and transmission rate.

4.2.1. Outage Probability

Since the concept of outage probability is discussed in detail in [**65**], this section will simply summarize its application to the current work. Again, the time index, t will be omitted during this discussion as the outage probability will be calculated at each transmission time-slot. Also, note that ε_i refers to the probability of loss of the transmission to user i in the current time-slot. All packets, m_i, transmitted to user i during the current time-slot will have a packet loss probability, ϵ_{m_i}, equal to ε_i. Using the model derived in [**65**], the probability of loss of a transmission to user i can be written as,

$$\begin{aligned} \varepsilon_i &= Prob(n_i B \log(1 + \tfrac{p_i h_i}{n_i}) \leq r_i), \\ &= Prob(h_i \leq \tfrac{n_i}{p_i} 2^{\frac{r_i}{n_i B}} - 1, \\ &= F_{x|e_i}(h_i|e_i), \end{aligned} \tag{4.5}$$

where, as in Chapter 2, B denotes the maximum symbol rate per code, and h_i denotes the instantaneous channel fading state (SINR per unit power) at that time-slot. $F_{x|e_i}$ denotes the

cumulative probability density function of the instantaneous channel fading state conditioned on the observed channel estimate, e_i. It is plain from (4.5) that the probability of loss, ε_i depends on 4 factors; the allocated resources (n_i, p_i), the estimated channel SINR (e_i), the assigned transmission rate (r_i), and the conditional cumulative density function given by the wireless channel model ($F_{x|e_i}$).

4.2.2. Wireless Channel Model

This work assumes that only partial (imperfect) channel state information is available at the scheduler/transmitter. Errors in the channel estimate can arise from the delay in the feedback channel combined with Doppler spread and quantization errors. It is possible to empirically determine the conditional cdf of the channel SINR conditioned on the channel estimate and the feedback delay using channel measurements. For the purposes of this work, the simulated channel traces obtained from Motorola were used to determine the statistics of the channel.

Figure 4.1 shows the probability density function obtained using a histogram of the simulated channel traces. The channel estimates are quantized into 64 non-uniform quantization levels using a Max-Lloyd quantizer. The x-axis denotes the available channel state estimate, and the y-axis denotes the probability density of the actual channel realization after 2msecs have elapsed from the channel measurement. The figure shows that the confidence in the channel estimate diminishes (i.e., the variance of the distribution increases) as the value of the estimate increases. Armed with the analysis in Fig. 4.1, the distribution of the channel, $F_{x|e_i}$, can be tabulated for each value of the channel estimate, e_i.

It is also possible to use an analytical channel model in the context of this work. For example, a commonly used channel fading model in similar setups is that of Nakagami-m

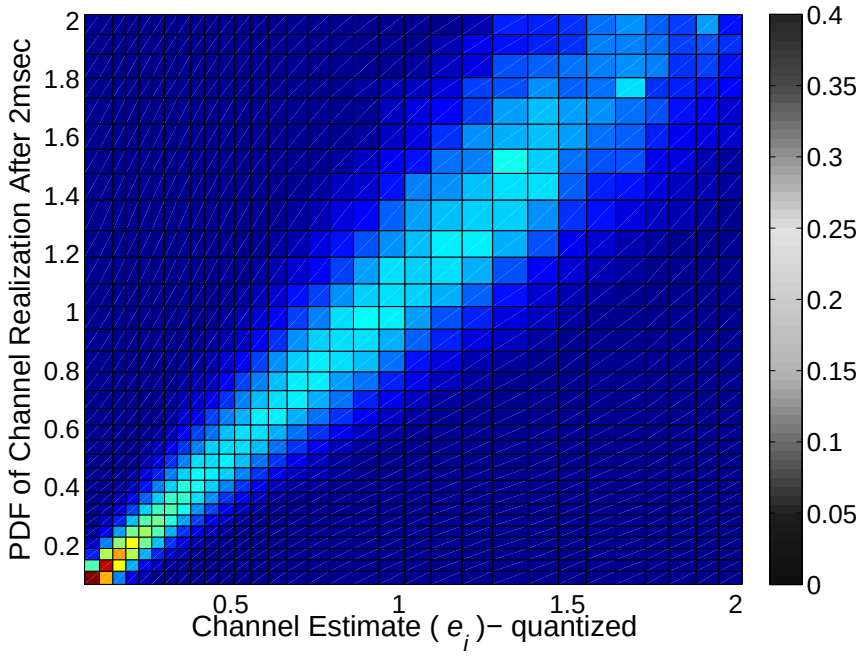

Figure 4.1. Empirical PDF of Channel SINR Given Delayed Estimate

fading. In that case, the channel SINR distribution can be modeled as a gamma distribution with mean at the channel estimate, e_i. The cumulative probability density function can be written as,

$$F_{x|e_i}(h_i) = \frac{\gamma(m, \frac{mh_i}{e_i})}{\Gamma(m)}, \tag{4.6}$$

where m is a shape parameter determined by the order, m, of the Nakagami-m distribution, $\gamma()$ denotes an incomplete gamma function, and $\Gamma(m)$ denotes the gamma function of order m. Figure 4.2 illustrates a few possible distributions using Nakagami fading models of different order and mean. Note that for a fixed order, m, the variance of the distribution increases with increasing mean (i.e., channel estimate).

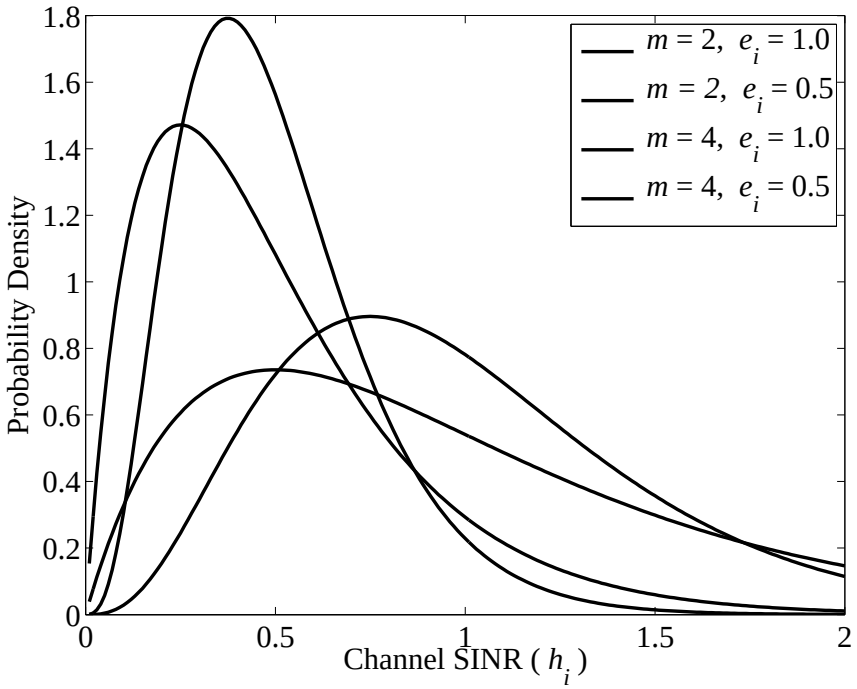

Figure 4.2. Nakagami fading with order m and mean at e_i

4.2.3. Problem Formulation

Given the packet ordering scheme, and method for calculating the loss probability described above, the scheduler jointly optimizes the rate assignment, $\mathbf{r} = (r_1, r_2, ..., r_K)$, where K is the number of users, the power assignment, $\mathbf{p} = (p_1, p_2, ..., p_K)$, and the spreading code assignment, $\mathbf{n} = (n_1, n_2, ..., n_K)$, in order to minimize the expected distortion in the system at each time slot. Let the expected distortion of the frame currently being transmitted to user i given the packet ordering specified in Sec. 4.1.2 be ED_i, obtained as in 4.2. Then, the optimization problem can be written as,

$$\min_{\mathbf{n},\mathbf{p},\mathbf{r}} \sum_{i=1}^{K} ED_i[r_i, \varepsilon_i(n_i, p_i, r_i, e_i)], \tag{4.7}$$

such that,

$$0 \leq \sum_{i=1}^{K} n_i \leq N, \quad 0 \leq n_i \leq N_i, \ \forall i, \tag{4.8}$$

$$0 \leq \sum_{i=1}^{K} p_i \leq P, \ \forall i, \tag{4.9}$$

and,

$$0 \leq \frac{p_i e_i}{n_i} \leq \hat{S}_i, \ \forall i. \tag{4.10}$$

In (4.10), $\hat{S}_i$ is a maximum SINR constraint [**26**]. The solution to (4.7), however, is not trivial, as an analytical form for ED_i, which will satisfy different video content and channel conditions, cannot be easily derived. Therefore, a two-step approach is used to tackle the problem.

As a first step, observe that for a given probability of loss, $\tilde{\varepsilon}_i$, and channel estimate, e_i, the rate assignment, r_i, must be a function of n_i and p_i as specified in (4.5). To further simplify the implementation of this step, ED_i is linearized, and then, for the fixed value of $\tilde{\varepsilon}_i$, the problem,

$$\max_{\mathbf{n},\mathbf{p}} \sum_{i=1}^{K} -\frac{\partial}{\partial r_i} ED_i[r_i(n_i, p_i, \tilde{\epsilon}_i, \tilde{\epsilon}_i] \cdot r_i(n_i, p_i, \tilde{\epsilon}_i), \tag{4.11}$$

is solved subject to the constraints in (4.8), (4.9), and (4.10). Here, $\partial/\partial r_i$ denotes the partial derivative with respect to r_i. Note that the gradient of ED_i with respect to r_i for a fixed probability of loss can be numerically calculated using the methods described in Sec. 4.1.2,

and the formulation described in Sec. 2.2. The solution to the type of problem in (4.11) can be found in [**26**].

For the second step, it can be observed that when n_i and p_i are fixed, then ε_i is a function of only r_i, and ED_i becomes a convex function of r_i. Since there is no multiuser constraint on the r_i assignment for a given user, the following convex optimization problem can be solved separately for each user i with a simple one-dimensional line search.

$$\min_{r_i} ED_i[r_i, \epsilon_i(\hat{n}_i, \hat{p}_i, r_i, e_i)], \tag{4.12}$$

where $\hat{n}_i$ and $\hat{p}_i$ are the values of n_i and p_i found in the solution to (4.11).

4.3. Simulation Results

Six video sequences with varied content (foreman, carphone, mother and daughter, news, hall monitor, and silent), in QCIF (176x144) format were used for the simulations. The video sequences were encoded in H.264 (JVT reference software, JM 10.2 [**68**]) at variable bit rates to obtain a decoded PSNR of 35dB at each frame. All frames except the first were encoded as P frames. To reduce error propagation due to packet losses, 15 random I MBs were inserted into each frame, and constrained intra prediction was used at the encoder. The frames were packetized such that each slice contained one row of MBs, which enabled a good balance between error robustness, and compression efficiency.

The wireless network was modeled as an HSDPA system with similar parameters to those specified in the previous chapters (Table 2.1. Realistic channel traces for an HSDPA system were obtained using a proprietary channel simulator developed at Motorola Inc. The channel traces were used to obtain the channel fading model as depicted in Fig. 4.1. The channel

feedback delay was set at 4 msec. It was also assumed that an ACK/NACK feedback for transmitted packets was available with a feedback delay of 10 msec.

The simulations compare three different methods for determining the resource allocation. They are:

(1) Expected Distortion Gradient - This is the proposed content-aware method as described in Sec. 4.2.

(2) Expected Distortion Gradient with Fixed Loss - In this method, packet ordering is performed using the expected distortion as specified in Sec. 4.1.2 but in the resource allocation, the probability of loss, ε_i is fixed for all users. Essentially, this method eliminates the second step of the solution in Sec. 4.2, and thus, is less computationally complex than the first.

(3) Queue Length - This method is not content-aware and uses the queue lengths at each user's transmission buffer [**24**] to determine the resource allocation. As in the second method, this also assumes a fixed ε_i for all users. The main difference between this method and the second is that in this method, the packets are not ordered according to their expected distortion gradients.

Figure 4.3 shows the average quality of the received video of each user, after scheduling and transmission over a packet lossy network, using the three different schemes. The results are averaged over each video sequence and 5 channel realizations. For the fixed loss schemes, ε_i is fixed at 0.1 for all users. The figure shows that the proposed content-dependent schemes significantly outperform the queue-length dependent scheme in terms of average received quality.

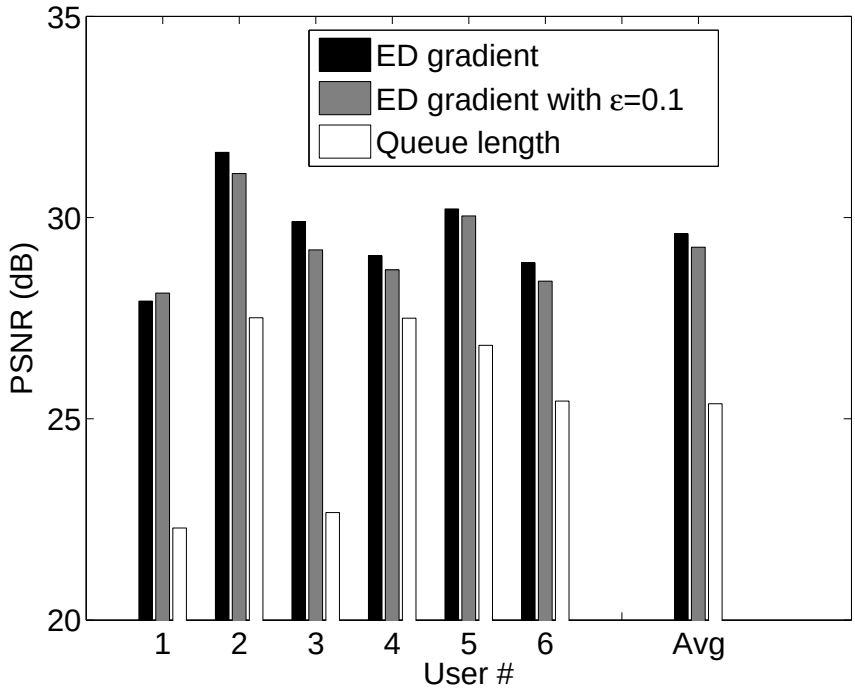

Figure 4.3. Average received PSNR

Figure 4.4 and 4.5 show the variance of the received PSNR using the three different schemes. Figure 4.4 shows the variance of quality at each video frame across all users and channel realizations. The queue length scheme shows a significantly larger variance across users than the others. quality at each frame over the users and channel realizations. These results can be attributed partly to the packet ordering and also to the fact that the queue length dependent scheme does not consider the concealability of video packets when allocating resources across users. Therefore, assuming two users have equal queue lengths, the user who receives video packets, that are difficult to conceal if lost, will not be given priority over the other user. Figure 4.5 shows the variance of quality across all video frames of the sequence and multiple channel realizations averaged over all the users. This represents the variability in quality experienced by each user during a given transmission session. Again,

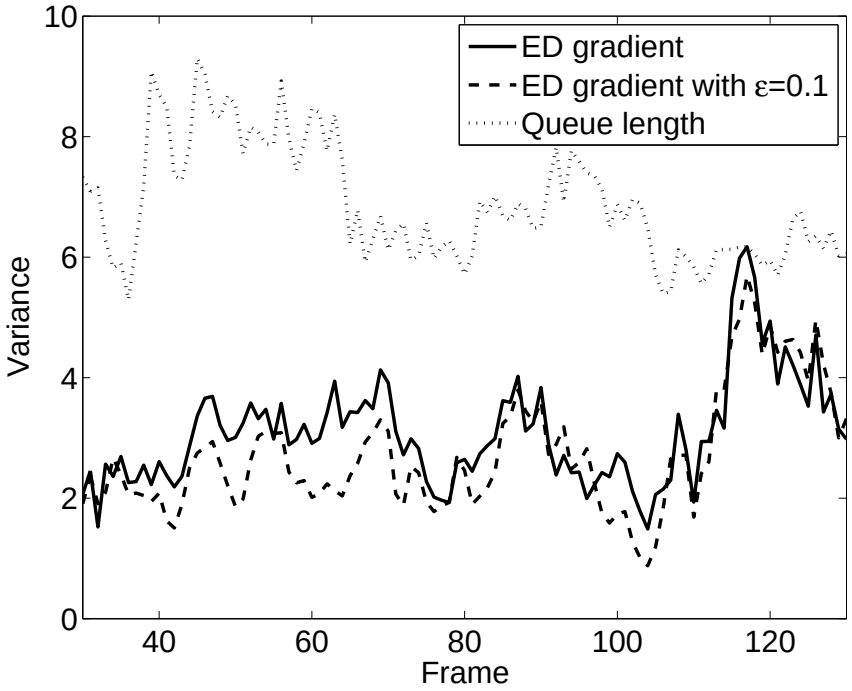

Figure 4.4. Received PSNR variance across users

the queue length method shows a significantly higher variance. Also, the expected distortion gradient method with fixed probability of loss shows a higher variance than the first method that optimizes over the probability of loss.

Figures 4.6 and 4.7 show the variation in average received PSNR as the value of ε_i is varied for the two schemes that use a fixed probability of loss. Figure 4.6 shows the results for the content-aware scheme, and it is apparent that the overall video quality remains within a 0.5dB range over a large range of ε. This result shows that the choice of ε does not significantly affect the performance of the system for the content-aware case. Figure 4.7 shows the results for the queue length scheme. In this case, the choice of ε does have an impact on the average received PSNR.

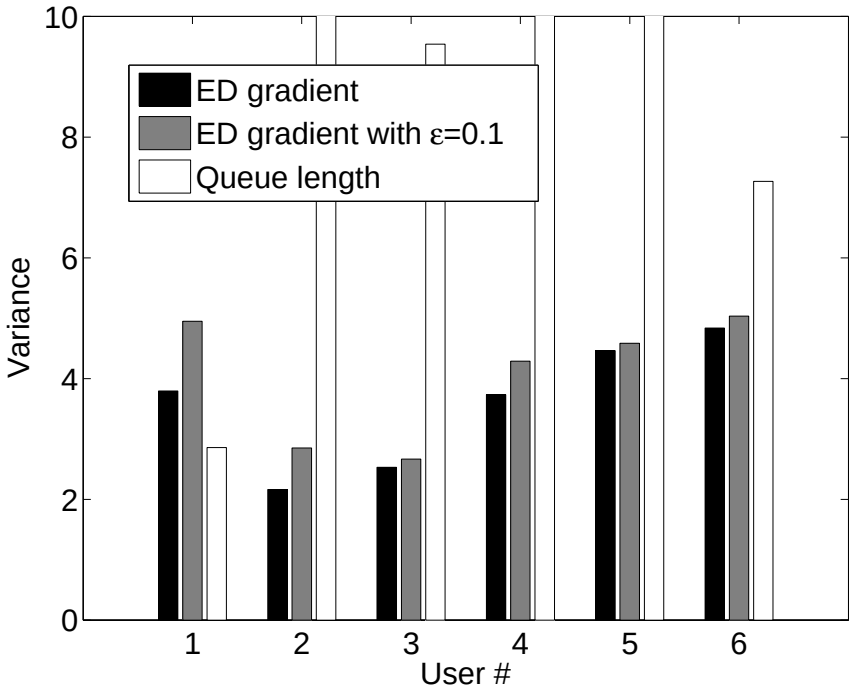

Figure 4.5. Received PSNR variance across frames of each user's sequence and averaged over all users

4.4. Conclusions

This chapter introduces a content-aware multi-user resource allocation and packet scheduling scheme that can be used in wireless networks where only imperfect channel state information is available at the scheduler. The scheme works by jointly optimizing the resource allocation and channel error protection in a content-aware manner while also prioritizing video packets in the transmission queue. The scheme significantly outperforms a conventional content-independent scheduling scheme.

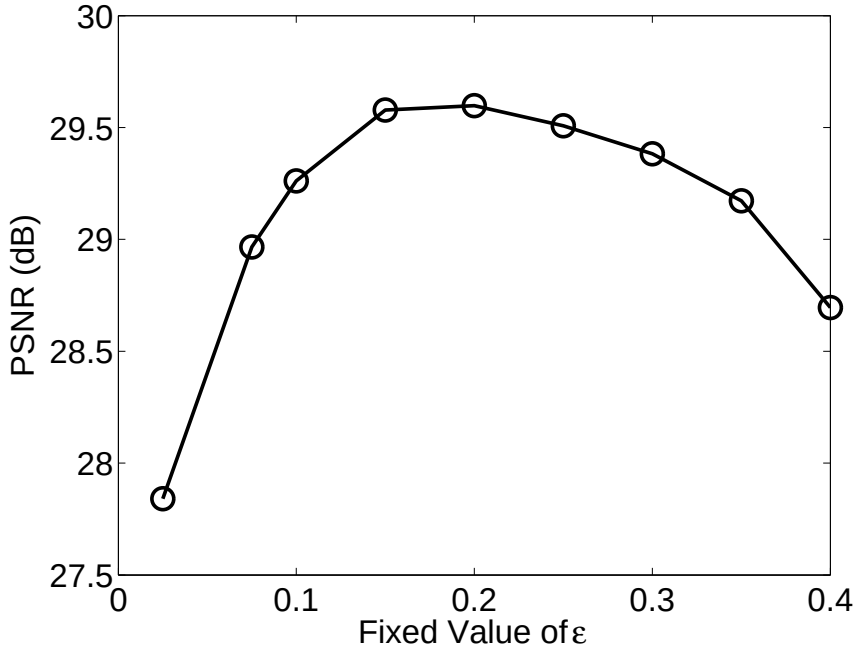

Figure 4.6. Sensitivity of received quality to choice of ε_i when using expected distortion gradient scheme with fixed ε_i.

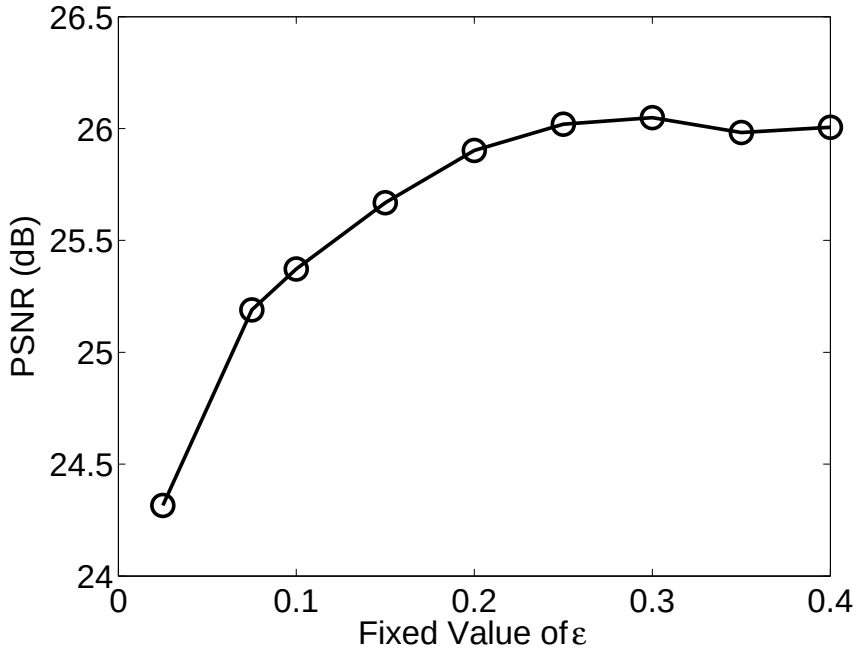

Figure 4.7. Sensitivity of received quality to choice of ε_i when using queue length based scheme with fixed ε_i

CHAPTER 5

Conclusions and Future Work

5.1. Summary and Conclusions

This dissertation addresses the problem of video packet scheduling and resource allocation for downlink video transmission in multiuser wireless networks. The first chapter discusses the scope of the problem, and provides some background on the advancements in wireless access technologies, video compression standards, and scheduling theory, that have lead the way for the proposed solutions in this work.

In the second chapter, the general scheduling and resource allocation framework is discussed in detail, with simulations showing the performance gains that can be expected by using the distortion based utilities for resource allocation and scheduling. The simulations using varied video content shows the value of using content-dependent techniques instead of the conventional content-independent techniques for resource allocation. An overall performance gain of over 3dB PSNR can be achieved by using the proposed techniques. An investigation of the use of a more complicated video error concealment technique shows that taking the complicated decoder error concealment into account at the scheduler can also be beneficial in terms of performance. It is also important to note that the distortion based metric calculations, when performed offline with less knowledge of the channel characteristics, can still outperform the content-independent metrics.

The use of scalable video coding techniques is discussed in the second chapter with special emphasis on the hierarchical bi-prediction and fine granularity scalability methods

that have been developed in recent standardization efforts. It is shown that efficient packet scheduling strategies can be used with scalable video coding in order to make scalable coded video bitstreams more amenable to the gradient based scheduling techniques discussed in Chapter 2. Again, it is shown that content dependent resource allocation can outperform the content-independent techniques especially under high network load. Comparisons between conventionally coded video and scalable coded video show that scalable coded video tends to outperform conventionally coded video under most circumstances unless the conventionally coded video bitrates are tuned perfectly to the prevailing channel conditions.

In Chapter 4, the problem is discussed in the context of imperfect channel state information, when random packet losses can occur in the channel. A two step approach to solving the resource allocation problem is presented in which at the first step, the probability of packet loss in the channel is kept constant and the resource allocation parameters are found, and in the next step, the optimal rate allocation over the users, given the resource allocation, is obtained. Again, the content-dependent schemes are shown to be more robust to channel losses than the content-independent schemes, and show a significant performance gain.

5.2. Future Work

The methods discussed in this work to make use of opportunistic scheduling and resource allocation techniques in a content-dependent manner can be applicable to many other scenarios in addition to downlink video streaming. This section discusses some of the applications and potentials for future work based on this work.

5.2.1. Uplink Video Transmission

Applications such as uploading of video content to a centralized server, video conferencing, and video surveillance over wireless networks are among the potential applications that will benefit from the increased throughput offered by emerging fourth generation wireless networks. In this setting, an important problem will be that of providing high quality of service on the wireless uplink. Most uplink video applications will also require real-time video encoding at the mobile client. Therefore, joint source and channel coding methods can be envisioned in which the source and channel coding schemes adapt in real-time to the prevailing channel conditions as well as transmitted video content. Important factors such as exploiting multiuser diversity, maintaining fairness across users, controlling congestion, reducing latency and increasing error resilience, must be taken into account when devising the source and channel resource allocation strategies for multiuser wireless video communication.

Dynamic channel and network conditions as well as the need to adapt the video encoding in real-time, make the opportunistic scheduling and resource allocation methods discussed in this work an attractive basis for research in uplink video transmission as well. In the uplink case, however, the encoded packets will only be contained at the client, and therefore, information on each user's content will not be immediately available at the base station. Emerging wireless technologies such as WiMAX [**14**] are leaning towards polling based mechanisms to determine the resource allocations for each client. In order to perform content-adaptive resource allocation, the information on each user's content will need to be communicated by each client to the MAC scheduler at the wireless base station. Therefore, efficient methods will need to be developed for communicating content-specific information

(eg., distortion-based utility functions, delay deadlines) to the base station. Once such information is available content-dependent gradient-based resource allocation strategies such as those proposed in this dissertation can be adapted to the uplink case as well.

In uplink video transmission, the base station will not have access to sufficient information on the video content in order to perform a joint optimization over both the scheduling and resource allocation. Therefore, the two may need to be performed separately. One possible approach to tackle this problem would be for the mobile user to assume a fixed packet loss rate during the packet scheduling. Then, the expected distortion gradients found using the fixed packet loss rates can be communicated to the base station, which can in turn reply with a resource allocation optimized over all the uplink users. The mobile client can then adapt its transmission rate to the resources allocated by the base station.

Another important problem in multiuser uplink video transmission with real-time video encoding is that of controlling the congestion in the wireless network. In video encoding, the rate distortion optimization at the video encoder assumes a certain bit budget is available for the encoding of a video frame (Note that the rate distortion optimization problem can also be formulated as one of minimizing the source rate subject to a maximum distortion.) Congestion control in the system can be achieved by adaptively changing the available bit budget (or inversely, the maximum tolerable distortion) for each client based on the measured user throughput for previous video frames. Naturally, this leads to two possible techniques, one which simultaneously reduces the bit budget for every user given the average throughput across all users, and the other, which performs a decentralized rate adaptation similar to the AIMD (Additive Increase Multiplicative Decrease) scheme used in TCP based congestion control. In the case of wireless data transmission, the choice of proper mechanism is further complicated by the fact that packet losses can occur due to both congestion and random

channel quality fluctuations. Therefore, the proper technique for congestion control is an important area for future study of uplink video transmission.

5.2.2. Video Transmission Over Mobile Ad Hoc Networks

Video transmission over mobile ad hoc wireless networks is another key area of research that can benefit from the scheduling and resource allocation techniques discussed in this work. Such networks can be used for military surveillance applications, for real-time video communications in disaster areas and search and rescue operations, and for civilian applications such as building and highway automation. Maintaining quality of service in such networks, however, is a challenging problem, and although it has received some attention in recent years, there are still many obstacles remaining to be overcome. This is especially true when dealing with congestion and fairness related issues for the transmission of multiple video streams over a mobile ad hoc wireless network.

Some of the challenges in this area are a result of the architecture of ad hoc wireless networks, which can consist of a mixture of fixed and mobile wireless nodes. Mobility implies that the routing and resource allocation in the network will need to dynamically adapt to changing conditions as links between nodes are established and removed depending on their changing locations, and time-varying channel conditions. Other challenges are a result of the video content. For example, real-time video traffic imposes stringent delay constraints that must be met for individual data packets. In addition to low delay, video traffic requires higher overall data throughput than other types of data, which is difficult to achieve given the low and time-varying data rates achievable in ad hoc wireless networks. Also, the data rate requirements are highly dependent on the particular video content being transmitted and can vary with each video flow. Therefore, the gradient-based scheduling

methods discussed in this work can provide a basis for overcoming the challenges related to the allocation of resources across users in ad hoc wireless networks such that fairness and high quality of service is maintained across multiple flows.

Current work in the area of cross-layer optimized video transmission for ad hoc wireless networks can be found in [**69, 70, 71, 72, 73, 74**] where the focus is on single user transmissions. Some initial work on multi-user video streaming over multi-hop wireless networks is presented in [**75**], this area of research is still far from complete. Also, it can be beneficial to consider strategies for multi-user video streaming that do not necessarily require prioritized encoding strategies such as scalable video coding.

The work in [**69, 70**], as well as many of the other current approaches to video streaming over ad hoc wireless networks, make use of simplified schemes to estimate the end-to-end distortion of the video. Generally, these schemes assume an additive distortion model in which each video packet has a known incremental contribution to the quality of the final video irrespective of the other packets available at the decoder. In reality, however, as demonstrated in this dissertation, error concealment techniques, which exploit spatial and temporal correlations among individual video packets can, and do, play an important role in determining the actual quality of the received video. Therefore, schemes that take complex error concealment techniques into account can potentially be of benefit in improving the performance of multihop video streaming applications as well.

In conclusion, it is apparent that the opportunistic content-dependent scheduling and resource allocation methods presented in this work can be of potential benefit for applications other than downlink video streaming as well. The problems related to real time video encoding and transmission, uplink video transmission, and video transmission over mobile ad

hoc networks can lead to some exciting new areas of research in multiuser video transmission over wireless networks.

References

[1] R. Berezdivin, R. Breinig, and R. Topp, "Next-generation wireless communications concepts and technologies," *IEEE Commun. Mag.*, vol. 40, no. 3, pp. 108–116, Mar. 2002.

[2] B. Girod, M. Kalman, Y. Liang, and R. Zhang, "Advances in channel-adaptive video streaming," *Wireless Communications and Mobile Computing*, vol. 2, no. 6, pp. 573–584, Sept. 2002.

[3] D. Wu, Y. Hou, and Y.-Q. Zhang, "Transporting real-time video over the internet," *Proc. IEEE*, vol. 88, no. 12, pp. 1855–1877, 2000.

[4] H. Zheng, "Optimizing wireless multimedia transmission through cross layer design," in *Proc. IEEE Int. Conf. on Multimedia and Expo*, Baltimore, MD, USA, May 2003.

[5] A. Katsaggelos, Y. Eisenberg, F. Zhai, R. Berry, and T. Pappas, "Advances in efficient resource allocation for packet-based real-time video transmission," *Proc. IEEE*, vol. 93, no. 1, pp. 135–147, Jan. 2005.

[6] Y. Wang, G. Wen, S. Wenger, and A. Katsaggelos, "Review of Error Resilient Techniques for Video Communications," *IEEE Signal Processing Magazine*, vol. 17, no. 4, pp. 61–82, July 2000.

[7] Y. Wang and Q.-F. Zhu, "Error control and concealment for video communication: a review," *Proc. IEEE*, vol. 86, pp. 974–997, May 1998.

[8] R. Zhang, S. L. Regunathan, and K. Rose, "Video coding with optimal inter/intra-mode switching for packet loss resilience," *IEEE Trans. Commun.*, vol. 18, pp. 966–976, June 2000.

[9] F. Zhai, Y. Eisenberg, T. Pappas, R. Berry, and A. Katsaggelos, "Joint source-channel coding and power adaptation for energy efficient wireless video communications," *Signal Processing: Image Communication*, vol. 20, pp. 371–387, 2005.

[10] T. Stockhammer, T. Wiegand, and S. Wenger, "Optimized transmission of H.26L/JVT coded video over packet-switched networks," in *Proc. IEEE Int. Conf. on Image Processing*, Rochester, NY, USA, Sept. 2002.

[11] *High Speed Downlink Packet Access; Overall Description*, 3GPP Std. TS 25.308 v7.0.0, 2006.

[12] E. Dahlman, P. Beming, J. Knutsson, F. Ovesjo, M. Persson, and C. Roobol, "WCDMA-the radio interface for future mobile multimedia communications," *IEEE Trans. on Vehicular Technology*, vol. 47, no. 4, pp. 1105–1118, 1998.

[13] T. Kolding, F. Frederiksen, and P. Mogensen, "Performance aspects of WCDMA systems with high speed downlink packet access HSDPA," in *Proc. IEEE Vehicular Technology Conference*, Fall 2002, pp. 477–481.

[14] *IEEE Standard for Local and Metropolitan Area Networks; Part 16: Air Interface for Fixed and Mobile Broadband Wireless Access Systems*, IEEE Std. 802.16e, 2005.

[15] C. Eklund, R. Marks, K. Stanwood, and S. Wang, "IEEE standard 802.16: A technical overview of the wirelessman air interface," *IEEE Communications Magazine*, vol. 40, no. 6, pp. 98–107, 2002.

[16] F. Frederiksen and R. Prasad, "An overview of OFDM and related techniques towards development of future wireless multimedia communications," in *IEEE Radio and Wireless Conference*, Aug 2002.

[17] R. Knopp and P. Humblet, "Information capacity and power control in single-cell multiuser communications," in *Proc. IEEE Int. Conf. on Communications*, vol. 1, Seattle, June 1995, pp. 331–335.

[18] S. Shakkottai, T. Rappaport, and P. Karlsson, "Cross-layer design for wireless networks," *IEEE Commun. Mag.*, vol. 41, no. 10, pp. 74–80, Oct. 2003.

[19] S. Lu, V. Bharghavan, and R. Srikant, "Fair scheduling in wireless packet networks," *IEEE/ACM Trans. on Networking*, vol. 7, no. 4, pp. 473–489, Aug. 1999.

[20] S. Shakkottai, R. Srikant, and A. Stolyar, "Pathwise optimality and state space collapse for the exponential rule," in *Proc. IEEE Int. Symp. on Information Theory*, Lausanne, Switzerland, June 2002, p. 379.

[21] Y. Liu, S. Gruhl, and E. Knightly, "Wcfq: An opportunistic wireless scheduler with statistical fairness bounds," *IEEE Trans. Wireless Commun.*, vol. 2, no. 5, pp. 1017–1028, Sept. 2003.

[22] P. Liu, R. Berry, and M. Honig, "Delay-sensitive packet scheduling in wireless networks," in *Proc. IEEE Wireless Communications and Networking*, vol. 3, New Orleans, LA, USA, Mar. 2003, pp. 1627–1632.

[23] A. Jalali, R. Padovani, and R. Pankaj, "Data throughput of CDMA-HDR a high efficiency - high data rate personal communication wireless system," in *Proc. VTC*, Spring 2000.

[24] M. Andrews, K. Kumaran, K. Ramanan, A. Stolyar, P. Whiting, and R. Vijayakumar, "Providing quality of service over a shared wireless link," *IEEE Commun. Mag.*, vol. 39, no. 2, pp. 150–154, Feb. 2001.

[25] A. Demers, S. Keshav, and S. Shenker, "Analysis and simulation of a fair queueing algorithm," in *Proc. ACM SIGCOMM*, 1989.

[26] R. Agrawal, V. Subramanian, and R. Berry, "Joint scheduling and resource allocation in CDMA systems," IEEE Trans. Inform. Theory, to appear.

[27] K. Kumaran and H. Viswanathan, "Joint power and bandwidth allocation in downlink transmission," *IEEE Trans. Wireless Commun.*, vol. 4, no. 3, pp. 1008–1016, May 2005.

[28] *Generic Coding of Moving Pictures and Associated Audio Information*, ISO/IEC Std. 13 818-2, 1995.

[29] T. Wiegand, G. Sullivan, G. Bjontegaard, and A. Luthra, "Overview of the H.264/AVC video coding standard," *IEEE Trans. on Circuits and Systems for Video Technology*, vol. 13, no. 7, pp. 560–576, 2003.

[30] *Draft ITU-T Recommendation and Final Draft International Standard of Joint Video Specification*, Std. ITU-T Rec. H.264—ISO/IEC 14 496-10 AVC, 2005.

[31] T. Stockhammer, M. Hannuksela, and T. Wiegand, "H.264/AVC in wireless environments," *IEEE Trans. on Circuits and Systems for Video Technology*, vol. 13, no. 7, pp. 657–673, 2003.

[32] T. Wedi, "Motion- and aliasing-compensated prediction for hybrid video coding," *IEEE Trans. on Circuits and Systems for Video Technology*, vol. 13, no. 7, pp. 577–586, 2003.

[33] P. List, A. Joch, J. Lainema, G. Bjontegaard, and M. Karczewicz, "Adaptive deblocking filter," *IEEE Trans. on Circuits and Systems for Video Technology*, vol. 13, no. 7, pp. 614–619, 2003.

[34] M. Flierl and B. Girod, "Generalized b pictures and the draft H.264/AVC video compression standard," *IEEE Trans. on Circuits and Systems for Video Technology*, vol. 13, no. 7, pp. 587–597, 2003.

[35] P. Topiwala, "Introduction and overview of scalable video coding (SVC)," in *Applications of Digital Image Processing XXIX*, A. G. Tescher, Ed., vol. 6312, no. 1. San Diego, CA, USA: SPIE, 2006, p. 63120Q.

[36] B. Pesquet-Popescu and V. Bottreau, "Three-dimensional lifting schemes for motion compensated video compression," in *IEEE Int. Conf. on Acoustics Speech and Signal Processing*, vol. 3, May 2001, pp. 1793–1796.

[37] H. Schwarz, D. Marpe, and T. Wiegand, "Overview of the scalable H.264/MPEG4-AVC extension," in *Proc. IEEE Int. Conf. on Image Processing*, Atlanta, GA, USA, Oct. 2006, pp. 161–164.

[38] H. Radha, M. van der Schaar, and Y. Chen, "The MPEG-4 fine-grained scalable video coding method for multimedia streaming over IP," *IEEE Trans. Multimedia*, vol. 3, pp. 53–68, Mar. 2001.

[39] W. Li, "Overview of fine granularity scalability in MPEG-4 video standard," *IEEE Trans. Circuits Syst. Video Technol.*, vol. 11, no. 3, pp. 301–317, Mar. 2001.

[40] "Robust mode selection for block-motion-compensated video encoding," Ph.D. Dissertation, Massachusetts Inst. Technology, Cambridge, MA, 1999.

[41] Z. He, J. Cai, and C. W. Chen, "Joint source channel rate-distortion analysis for adaptive mode selection and rate control in wireless video coding," *IEEE Trans. on Circuits and Systems for Video Technology*, vol. 12, no. 6, pp. 511–523, 2002.

[42] C. E. Luna, Y. Eisenberg, T. N. Pappas, R. Berry, and A. K. Katsaggelos, "Joint source coding and data rate adaptation for energy efficient wireless video streaming," *IEEE Journ. on Selected Areas in Communications*, vol. 21, no. 10, pp. 1710–1720, 2003.

[43] Y. Eisenberg, C. E. Luna, T. N. Pappas, R. Berry, and A. K. Katsaggelos, "Joint source coding and transmission power management for energy efficient wireless video communications," *IEEE Trans. Circuits and Systems for Video Technology*, vol. 12, no. 6, pp. 411–424, 2002.

[44] Y. Eisenberg, F. Zhai, T. N. Pappas, R. Berry, and A. K. Katsaggelos, "Vapor: Variance-aware per-pixel optimal resource allocation," *IEEE Trans. Image Processing*, vol. 15, no. 2, pp. 289–299, 2006.

[45] P. Chou and Z. Miao, "Rate-distortion optimized streaming of packetized media," *IEEE Trans. Multimedia*, vol. 8, no. 2, pp. 390–404, Apr. 2006.

[46] J. Chakareski, P. Chou, and B. Aazhang, "Computing rate-distortion optimized policies for streaming media to wireless clients," in *Proc. Data Compression Conference*, Apr 2002, pp. 53–62.

[47] Z. Miao and A. Ortega, "Optimal scheduling for streaming of scalable media," in *Proc. Asilomar*, Nov. 2000.

[48] Y. Ofuji, S. Abeta, and M. Sawahashi, "Unified Packet Scheduling Method Considering Delay Requirement in Forward Link Broadband Wireless Access," in *IEEE Vehicular Technology Conference*, Fall 2003.

[49] P. Falconio and P. Dini, "Design and Performance Evaluation of Packet Scheduler Algorithms for Video Traffic in the High Speed Downlink Packet Access," in *Proc. of PIMRC 2004*, Sept. 2004.

[50] D. Kim, B. Ryu, and C. Kang, "Packet Scheduling Scheme for real time Video Traffic in WCDMA Downlink," in *Proc. of 7th CDMA International Conference*, Oct. 2002.

[51] R. Tupelly, J. Zhang, and E. Chong, "Opportunistic Scheduling for Streaming Video in Wireless Networks," in *Proc. of Conference on Information Sciences and Systems*, 2003.

[52] G. Liebl, T. Stockhammer, C. Buchner, and A. Klein, "Radio link buffer management and scheduling for video streaming over wireless shared channels," in *Proc. Packet Video Workshop*, 2004.

[53] G. Liebl, M. Kalman, and B. Girod, "Deadline-aware scheduling for wireless video streaming," in *Proc. IEEE Int. Conf. on Multimedia and Expo*, July 2005.

[54] G. Liebl, T. Schierl, T. Wiegand, and T. Stockhammer, "Advanced wireless multiuser video streaming using the scalable video coding extensions of H.264/MPEG4-AVC," in *Proc. IEEE Int. Conf. on Multimedia and Expo*, 2006.

[55] H. Schwarz, D. Marpe, and T. Wiegand, "Analysis of hierarchical B pictures and MCTF," in *Proc. IEEE Int. Conf. on Multimedia and Expo*, 2006.

[56] J. Huang, V. Subramanian, R. Agrawal, and R. Berry, "Downlink Scheduling and Resource Allocation for OFDM Systems," in *Conference on Information Sciences and Systems (CISS 2006)*, March 2006.

[57] "JVT reference software," http://iphome.hhi.de/suehring/tml/download, JM 9.3.

[58] M. Hong, L. Kondi, H. Schwab, and A. Katsaggelos, "Error Concealment Algorithms for Concealed Video," *Signal Processing: Image Communications, special issue on Error Resilient Video*, vol. 14, no. 6-8, pp. 437–492, 1999.

[59] Y.-K. Wang, M. Hannuksela, V. Varsa, A. Hourunranta, and M. Gabbouj, "The Error Concealment Feature in the H.26L Test Model," in *Proc. IEEE Int. Conf. on Image Processing (ICIP)*, 2002.

[60] S. Belfiore, M. Grangetto, E. Magli, and G. Olmo, "Spatio-Temporal Video Error Concealment with Perceptually Optimized Mode Selection," in *Proc. IEEE Int. Conf. on Acoustics Speech and Signal Processing (ICASSP)*, vol. 5, 2003, pp. 748–751.

[61] T. Wiegand, G. Sullivan, J. Reichel, H. Schwarz, and M. Wien, "Joint draft 6," JVT-S201, 19th JVT Meeting, Geneva, CH, 2006.

[62] S. Wenger, Y.-K. Wang, and T. Schierl, "RTP payload format for SVC video," Internet Draft, IETF, Oct. 2006.

[63] "JSVM 4 reference software," JVT-Q203, Nice, France, Oct. 2005.

[64] P. Pahalawatta, R. Berry, T. Pappas, and A. Katsaggelos, "A content-aware scheduling scheme for video streaming to multiple users over wireless networks," in *Proc. European Signal Processing Conference*, Florence, Italy, Sept. 2006.

[65] L. Ozarow, S. Shamai, and A. Wyner, "Information theoretic considerations for cellular mobile radio," *IEEE Trans. on Vehicular Technology*, vol. 43, no. 2, pp. 359–378, 1994.

[66] H. Yang and K. Rose, "Advances in recursive per-pixel estimation of end-to-end distortion for application in H.264," in *Proc. IEEE Int. Conf. on Image Processing (ICIP)*, Genova, Sept. 2005.

[67] D. Wu, Y. T. Hou, B. Li, W. Zhu, Y. Q. Zhang, and H. J. Chao, "An end-to-end approach for optimal mode selection in internet video communication: theory and application," *IEEE Trans. Commun.*, vol. 18, pp. 977–995, June 2002.

[68] "JVT reference software," http://iphome.hhi.de/suehring/tml/download, JM 10.2.

[69] E. Setton, T. Yoo, X. Zhu, A. Goldsmith, and B. Girod, "Cross-layer design of ad hoc networks for real-time video streaming," *IEEE Wireless Communications*, pp. 59–65, Aug. 2005.

[70] E. Setton, X. Zhu, and B. Girod, "Congestion-optimized multi-path streaming of video over ad hoc wireless networks," in *Proc. IEEE Int. Conf. on Multimedia and Expo*, 2004.

[71] Y. Andreopoulos, N. Mastronarde, and M. V. der Schaar, "Cross-layer optimized video streaming over wireless multihop mesh networks," *IEEE Journal on Selected Areas in Communications*, vol. 24, no. 11, pp. 2104–2115, Nov. 2006.

[72] Q. Li and M. V. der Schaar, "Providing adaptive qos to layered video over wireless local area networks through real-time retry limit adaptation," *IEEE Trans. on Multimedia*, vol. 6, no. 2, pp. 278–290, Apr. 2004.

[73] Y. Andreopoulos, R. Keralapura, M. V. der Schaar, and C.-N. Chuah, "Failure-aware open-loop adaptive video streaming with packet-level optimized redundancy," *IEEE Trans. on Multimedia*, vol. 8, no. 6, pp. 1274–1290, Dec. 2006.

[74] M. Wang and M. V. der Schaar, "Operational rate-distortion modeling for wavelet video coders," *IEEE Trans. on Signal Processing*, vol. 54, no. 9, pp. 3505–3517, Sept. 2006.

[75] H.-P. Shiang and M. van der Schaar, "Multi-user video streaming over multi-hop wireless networks: A distributed, cross-layer approach based on priority queueing," *IEEE Journal on Selected Areas in Communications: Special Issue on Cross-Layer Optimized Wireless Multimedia Communications*, vol. 25, no. 4, pp. 770–785, May 2007.